arXiv:1605.02607v1 [cs.IT] 9 May 2016

Convolutive superposition for multicarrier cognitive radio systems

Donatella Darsena, Giacinto Gelli, and Francesco Verde

Abstract

Recently, we proposed a spectrum-sharing paradigm for single-carrier cognitive radio (CR) networks, where a secondary user (SU) is able to maintain or even improve the performance of a primary user (PU) transmission, while also obtaining a low-data rate channel for its own communication. According to such a scheme, a simple multiplication is used to superimpose one SU symbol on a block of multiple PU symbols. The scope of this paper is to extend such a paradigm to a multicarrier CR network, where the PU employs an orthogonal frequency-division multiplexing (OFDM) modulation scheme. To improve its achievable data rate, besides transmitting over the subcarriers unused by the PU, the SU is also allowed to transmit multiple block-precoded symbols in parallel over the OFDM subcarriers used by the primary system. Specifically, the SU convolves its block-precoded symbols with the received PU data in the time-domain, which gives rise to the term *convolutive superposition*. An information-theoretic analysis of the proposed scheme is developed, which considers different amounts of network state information at the secondary transmitter, as well as different precoding strategies for the SU. Extensive simulations illustrate the merits of our analysis and designs, in comparison with conventional CR schemes, by considering as performance indicators the ergodic capacity of the considered systems.

Index Terms

Cognitive radio, channel capacity, multicarrier modulation, superposition, precoding design.

I. Introduction

Due to the explosive growth in wireless data services, mainly driven by video communications, next-generation wireless systems will require significant advances [1], [2] in terms of data-rate, latency, and energy consumptions, as well as improved networking and resource allocation procedures. Moreover, according to the emerging "Internet of Things" (IoT) paradigm and the diffusion of machine-to-machine communications, next-generation wireless systems must be able to support an enormous number of low-rate devices, which will require new approaches and policies for spectrum allocation and management, including new forms of *spectrum sharing*, where *cognitive radio* (CR) approaches [3], [4] are expected to play a major role. In CR techniques, secondary users (SUs) share a portion of the spectrum with licensed or unlicensed primary users (PUs). Such an approach is beneficial, e.g., for ultradense wireless systems [5], where medium-to-low-rate SU terminals might share the spectrum with high-rate PU devices.

D. Darsena is with the Department of Engineering, Parthenope University, Naples I-80143, Italy (e-mail: darsena@uniparthenope.it). G. Gelli and F. Verde are with the Department of Electrical Engineering and Information Technology, University Federico II, Naples I-80125, Italy [e-mail: (gelli,f.verde)@unina.it].

The cognitive radio approach stems from the fact that a major part of the licensed and unlicensed spectrum is typically unused for significant periods of time, so called *spectrum holes* or *white spaces*. Therefore, a simple opportunistic access paradigm consists of allowing the SUs to transmit in an orthogonal fashion (space, time or frequency) relative to the PU signals, which will be referred to as *orthogonal CR (OCR)*. [3], [4]. Such an approach requires a possible multidimensional space-time-frequency detection of PU users, called *spectrum sensing* [3], [4]. However, accurate detection of a vacant spectrum is not an easy task [6]. Moreover, next-generation wireless systems mandate non-orthogonal primary and secondary transmissions [1], which will be referred to as *non-orthogonal CR (NOCR)*.

There are two different visions in CR to accomplish spectrum sharing on a non-orthogonal basis [3], [4]: (i) SUs can share PU communications resources, provided that they keep the interference to PU transmissions (so called *interference temperature* [3]) below a very low threshold; (ii) sophisticated encoding and decoding techniques are used to remove all (or part of) the mutual interference between PU and SU transmissions [7]–[10], in order to relax the threshold on the SU transmission powers. In the former paradigm, one of the major problem is to determine the interference level a secondary transmitter causes to a primary receiver; in the latter one, sophisticated encoding techniques like dirty paper coding (DPC) [11] require *a priori* knowledge of the primary user's transmitted data and/or how this sequence is encoded (codebook). The underlying common feature of both approaches is the *additive superposition* of PU and SU transmissions (additive interference channel [9]), i.e, PU and SU signals add up.

Recently, we have proposed in [12], [13] a different NOCR paradigm where the arithmetic operation of multiplication is used to superimpose a single SU symbol on a primary signal composed of multiple PU symbols, through a single-channel amplify-and-forward (AF) protocol. The main advantages of such a scheme can be summarized as follows: (i) under non-restrictive conditions [13], the SU can transmit without a power constraint, while keeping the desirable property of not degrading (but even improving) the PU performance; (ii) *a priori* knowledge of the PU data at the SU is not required. However, the main limitation of the single-channel approach in [12], [13] is that only low-data rates can be achieved by the SU.

The aim of this paper is to improve the achievable data rates of the SU by introducing the concept of *convolutive superposition*, whereby the SU data are superimposed on the PU received signal by means of a time-domain convolution. Such a new code construction extends the multiplicative

superposition scheme of [12], [13] along three lines:[1]

1) We consider a CR system where modulation is based on *orthogonal frequency-division multiplexing (OFDM)* [14], due to its advantages in multipath resistance, performance, spectral efficiency, flexibility, and computational complexity. The multicarrier nature of the PU transmission allows the SU to be active over multiple primary subchannels, thereby attaining larger transmission rates compared to the single-channel scheme considered in [12], [13].
2) For each PU subchannel, we allow the SU to transmit multiple symbols within a single OFDM symbol interval of the primary system, by jointly exploiting both white spaces (i.e., unused subcarriers of the PU signal) and dirty spaces (i.e., subcarriers used by the PU).
3) The multi-channel multi-symbol nature of the secondary transmission introduces additional degrees of freedom with respect to the single-channel approach of [12], [13]: the distribution of the available power over the transmit dimensions. In this regard, we develop *precoding* strategies for the SU transmission by considering either the case when channel state information (CSI) is available at the secondary transmitter or this knowledge is missing.

The theoretical performance analysis of the proposed scheme is based on input-output mutual information and ergodic capacity of both the primary and secondary systems.[2] Results of comparisons studies with other CR approaches are also reported in terms of ergodic capacity.

The paper is organized as follows. The system model and the considered communication scheme are described in Section II. The capacity analysis for the PU is carried out in Section III. The information-theoretic analysis and precoding designs for the SU are developed in Section IV, by considering different amounts of CSI at both ends of the communication link. Numerical results are reported in Section V, aimed at corroborating our theoretical findings. Finally, the main results obtained in the paper are summarized in Section VI.

II. The considered cognitive radio system model

We consider a multicarrier cognitive network (see Fig. 1) composed by a primary transmitter-receiver pair (nodes PTx and PRx) and one secondary transmitter-receiver pair (nodes STx and

[1]Preliminary results of such an extension are reported in [15].

[2]The ergodic capacity serves as a useful upper bound on the performance of any communication system and it is to some extent amenable to analytic studies; it can be achieved if the length of the codebook is long enough to reflect the ergodic nature of fading (i.e., the transmission duration of the codeword is much greater than the channel coherence time) [16]. At rates lower than the ergodic capacity, there exist coding strategies ensuring that the average bit error rate (BER) decays exponentially with the codebook length [17], [18].

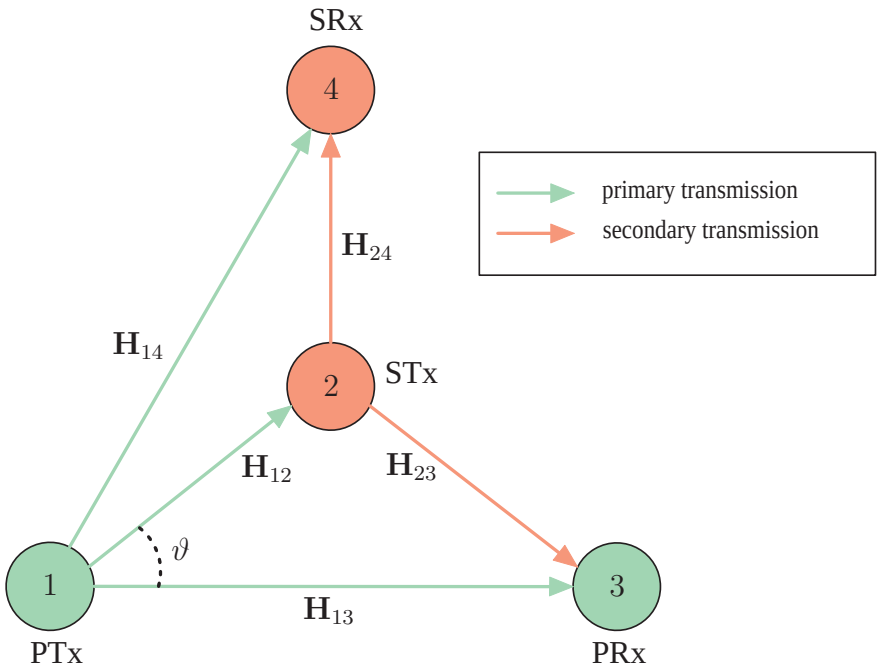

Figure 1. The wireless network model: in green, the PU transmitter/receiver nodes, in red the SU transmitter/receiver nodes.

SRx). The nodes have a single antenna and operate in half-duplex mode, except for the STx which is equipped with two antennas (one receive antenna and one transmit antenna) that enable a full-duplex operation.[3] The PU employs OFDM modulation with M subcarriers, a cyclic prefix (CP) of length $L_{\text{cp}} < M$, and symbol period $T_{\text{PU}} \triangleq P\,T_c$, where $P \triangleq M + L_{\text{cp}}$ and T_c denotes the sampling period of the PU system. Only Q out of the M available subcarriers are utilized, whereas the remaining $M_{\text{vc}} \triangleq M - Q > 0$ ones are unmodulated and called *virtual subcarriers (VCs)*. The STx exploits the PU transmission to deliver to the SRx its own data, by simultaneously transmitting over the same subcarriers of the PU, as described in Subsection II-C. It is assumed that the SU perfectly knows the allocation of the VCs within the PU frequency range.[4]

A. General assumptions regarding channels and noise

During an interval of duration T_{PU}, the wireless channel between the pair of nodes (i, j), for $i \in \{1, 2\}$ and $i \neq j \in \{2, 3, 4\}$, is modeled as a causal linear time-invariant (LTI) system spanning

[3]We assume that the transmit chain of the STx is adequately isolated from its receive chain [21], such that self-interference is negligible in the receive chain circuitry.

[4]Such a knowledge can be available *a priori* or obtained, e.g., by means of spectrum sensing techniques [3].

at the most $L_{ij} > 0$ sampling interval of the PU, i.e., its discrete-time impulse response obeys $\widetilde{h}_{ij}(\ell) \equiv 0$ for $\ell \notin \{0, 1, \ldots, L_{ij}\}$. Such an impulse response is fixed during the transmission of one OFDM symbol, but is allowed to independently change from one symbol to another.[5] In the sequel, we will denote with $\theta_{ij} \geq 0$ the integer time offset (TO) characterizing the $i \to j$ link (encompassing both the propagation delay of the wireless link and the processing time at node i), which models the fact that the receiver j does not know where the multicarrier blocks transmitted by node i start.[6] We will assume that, for each $i \to j$ link, the sum of the channel order and the TO turns out to be within one PU symbol, i.e., $L_{ij} + \theta_{ij} \leq P - 1$, such that the desired block received by node j is impaired only by the interblock interference (IBI) of the previous block. We also assume that each node is able to align its local oscillator to the carrier frequency of the received signal with negligible error. Hereinafter, with reference to a single PU symbol period, the frequency-domain channel matrix[7]

$$\boldsymbol{\mathcal{H}}_{ij} \triangleq \text{diag}[H_{ij}(0), H_{ij}(1), \ldots, H_{ij}(M-1)] \in \mathbb{C}^{M \times M} \tag{1}$$

with

$$H_{ij}(m) \triangleq e^{-j\frac{2\pi}{M}\theta_{ik}m} \sum_{\ell=0}^{L_{ik}} \widetilde{h}_{ij}(\ell)\, e^{-j\frac{2\pi}{M}\ell m}\,, \quad \text{for } m \in \mathcal{M} \triangleq \{0, 1, \ldots, M-1\} \tag{2}$$

collects the M-point discrete Fourier transform (DFT) of the *extended* channel impulse response $\widetilde{h}_{ij}(\ell - \theta_{ij})$ corresponding to the $i \to j$ link, with $\boldsymbol{\mathcal{H}}_{i_1 j_1}$ statistically independent of $\boldsymbol{\mathcal{H}}_{i_2 j_2}$ for $i_1 \neq i_2$ and $j_1 \neq j_2$; moreover, the diagonal entries of $\boldsymbol{\mathcal{H}}_{ij}$ are independent and identically distributed (i.i.d.) zero-mean circularly symmetric complex Gaussian (ZMCSCG) random variables (RVs) having variance σ_{ij}^2, which depends on the average path loss associated to the underlying link. In the PU symbol period $[nT_{\text{PU}}, (n+1)T_{\text{PU}})$, with $n \in \mathbb{Z}$, the vector $\widetilde{\mathbf{v}}_j(n) \in \mathbb{C}^P$ models the thermal noise at the jth receiver, with $j \in \{2, 3, 4\}$. We assume that $\widetilde{\mathbf{v}}_j(n)$ is a ZMCSCG random vector,

[5]For simplicity's sake, we will not explicitly indicate the dependence of the channels' parameters on the PU symbol period.

[6]The fractional TO is incorporated as part of $\{\widetilde{h}_{ij}(\ell)\}_{\ell=0}^{L_{ij}}$.

[7]An $n \times m$ matrix and a column vector over the field $\mathbb{F}$ are denoted as $\mathbf{A} \in \mathbb{F}^{n \times m}$ and $\mathbf{a} \in \mathbb{F}^n$, respectively; common fields are those of complex, real, and integer numbers, denoted with $\mathbb{C}$, $\mathbb{R}$, and $\mathbb{Z}$, respectively; $\mathbf{A}^{\mathrm{T}}$, $\mathbf{A}^{\mathrm{H}}$, $\mathbf{A}^{-1}$, $\mathbf{A}^{\dagger}$, and $\mathbf{A}^{-}$ denote the transpose, the conjugate transpose, the inverse, the Moore-Penrose generalized inverse [19], and the generalized (1)-inverse [19] of $\mathbf{A}$, respectively; $\mathbf{0}_m \in \mathbb{R}^m$, $\mathbf{O}_{m \times n} \in \mathbb{R}^{m \times n}$, and $\mathbf{I}_m \in \mathbb{R}^{m \times m}$ denote the zero vector, the zero matrix, and the identity matrix, respectively; for $\mathbf{a} \in \mathbb{C}^m$, $\mathbf{A} = \text{diag}(\mathbf{a}) \in \mathbb{C}^{m \times m}$ denotes the diagonal matrix whose diagonal elements are the entries of $\mathbf{a}$; $\mathbf{S}_{\text{f}} \in \mathbb{R}^{n \times n}$ and $\mathbf{S}_{\text{b}} \in \mathbb{R}^{n \times n}$ denote the Toeplitz "forward shift" and "backward shift" matrices [20], respectively, where the first column of $\mathbf{S}_{\text{f}}$ and the first row of $\mathbf{S}_{\text{b}}$ are given by $[0, 1, 0, \ldots, 0]^T$ and $[0, 1, 0, \ldots, 0]$, respectively; $\|\mathbf{a}\|$ is the Euclidean norm of $\mathbf{a} \in \mathbb{C}^m$; $\text{rank}(\mathbf{B})$ is the rank of $\mathbf{B} \in \mathbb{C}^{m \times n}$; $\det(\mathbf{B})$ denotes the determinant of $\mathbf{B} \in \mathbb{C}^{m \times m}$; $\mathsf{Prob}(A)$ denotes the probability of the event A; the operator $\mathsf{E}[\cdot]$ denotes ensemble mean and $\mathsf{E}[\cdot \mid A]$ is the conditional mean given the event A; finally, $x^+ \triangleq \max(x, 0)$.

with correlation matrix $\mathsf{E}[\widetilde{\mathbf{v}}_j(n)\,\widetilde{\mathbf{v}}_j^{\mathrm{H}}(n)] = \sigma_{v_j}^2\,\mathbf{I}_P$ and $\widetilde{\mathbf{v}}_{j_1}(n_1)$ statistically independent of $\widetilde{\mathbf{v}}_{j_2}(n_2)$ for $j_1 \neq j_2$ and $n_1 \neq n_2$. Finally, channel matrices, data transmitted by PU and SU, and noise vectors are statistically independent random objects.

B. Signal transmitted by the PTx

During the PU symbol period $[nT_{\mathrm{PU}}, (n+1)T_{\mathrm{PU}})$, the PTx transmits a frequency-domain symbol block $\mathbf{x}_{\mathrm{PU}}(n) \triangleq [x_{\mathrm{PU}}^{(0)}(n), x_{\mathrm{PU}}^{(1)}(n), \ldots, x_{\mathrm{PU}}^{(Q-1)}(n)]^{\mathrm{T}} \in \mathbb{C}^Q$ of Q symbols, modeled as i.i.d. zero-mean circularly symmetric complex RVs with variance P_{PU}, where $\mathsf{P}_{\mathrm{PU}} > 0$ is the PU power budget. We assume that CSI is not available at the PTx and, hence, P_{PU} is uniformly allocated across all data subcarriers. Vector $\mathbf{x}_{\mathrm{PU}}(n)$ is augmented by VCs insertion in arbitrary positions $\mathcal{I}_{\mathrm{PU,vc}} \triangleq \{q_0, q_1, \ldots, q_{M_{\mathrm{vc}}-1}\}$, thus obtaining the block $\mathbf{\Theta}\,\mathbf{x}_{\mathrm{PU}}(n)$, with $\mathbf{\Theta} \in \mathbb{R}^{M\times Q}$ modeling VCs insertion. Matrix $\mathbf{\Theta}$ or, equivalently, the set $\mathcal{I}_{\mathrm{PU,vc}}$ can be statically specified by the standard, or it can be dynamically adjusted to select the best Q available subcarriers, i.e., those with the highest signal-to-noise ratios (SNRs). Then, the block $\mathbf{\Theta}\,\mathbf{x}_{\mathrm{PU}}(n)$ is subject to conventional OFDM processing, encompassing M-point inverse discrete Fourier transform (IDFT), followed by CP insertion, thus obtaining (see, e.g., [22]) $\widetilde{\mathbf{u}}_{\mathrm{PU}}(n) = \mathbf{T}_{\mathrm{cp}}\,\mathbf{W}_{\mathrm{IDFT}}\,\mathbf{\Theta}\,\mathbf{x}_{\mathrm{PU}}(n)$, where $\mathbf{T}_{\mathrm{cp}} \triangleq [\mathbf{I}_{\mathrm{cp}}^{\mathrm{T}}, \mathbf{I}_M]^{\mathrm{T}} \in \mathbb{R}^{P\times M}$, with $\mathbf{I}_{\mathrm{cp}} \in \mathbb{R}^{L_{\mathrm{cp}}\times M}$ obtained from $\mathbf{I}_M$ by picking its last L_{cp} rows, and $\mathbf{W}_{\mathrm{IDFT}} \in \mathbb{C}^{M\times M}$ is the unitary symmetric IDFT matrix [22]. The entries of $\widetilde{\mathbf{u}}_{\mathrm{PU}}(n)$ are subject to digital-to-analog (D/A) plus radio-frequency (RF) conversion for transmission over the wireless channel.

C. Signal transmitted by the STx

Let $\widetilde{y}_2^{(p)}(n)$ denote the baseband-equivalent pth sample received by the STx within the nth PU symbol period, for $p \in \mathcal{P} \triangleq \{0, 1, \ldots, P-1\}$. By gathering such samples in the vector $\widetilde{\mathbf{y}}_2(n) \triangleq [\widetilde{y}_2^{(0)}(n), \widetilde{y}_2^{(1)}(n), \ldots, \widetilde{y}_2^{(P-1)}(n)]^{\mathrm{T}} \in \mathbb{C}^P$, the received signal can be expressed as

$$\widetilde{\mathbf{y}}_2(n) = \widetilde{\mathbf{H}}_{12}^{(0)}\,\widetilde{\mathbf{u}}_{\mathrm{PU}}(n) + \widetilde{\mathbf{H}}_{12}^{(1)}\,\widetilde{\mathbf{u}}_{\mathrm{PU}}(n-1) + \widetilde{\mathbf{v}}_2(n) \tag{3}$$

where we remember that $\widetilde{\mathbf{v}}_2(n)$ is the noise vector, whereas

$$\widetilde{\mathbf{H}}_{12}^{(0)} \triangleq \sum_{\ell=0}^{L_{12}} \widetilde{h}_{12}(\ell)\,\mathbf{S}_{\mathrm{f}}^{\ell+\theta_{12}} \in \mathbb{C}^{P\times P} \tag{4}$$

$$\widetilde{\mathbf{H}}_{12}^{(1)} \triangleq \sum_{\ell=0}^{L_{12}} \widetilde{h}_{12}(\ell)\,\mathbf{S}_{\mathrm{b}}^{P-\ell-\theta_{12}} \in \mathbb{C}^{P\times P} \tag{5}$$

are Toeplitz lower- and upper-triangular matrices, respectively.

In the proposed spectrum sharing scheme, the STx exploits the nth PU transmission to deliver to the SRx a frequency-domain block $\mathbf{x}_{\text{SU}}(n) \triangleq [x_{\text{SU}}^{(0)}(n), x_{\text{SU}}^{(1)}(n), \ldots, x_{\text{SU}}^{(N+M_{\text{vc}}-1)}(n)]^{\text{T}} \in \mathbb{C}^{N+M_{\text{vc}}}$, which is composed of $N + M_{\text{vc}}$ symbols, modeled as i.i.d. zero-mean unit-variance circularly symmetric complex RVs. It is assumed that $N + M_{\text{vc}} \leq M$ and, thus, the *rate* of the SU is $N + M_{\text{vc}}$ symbols per OFDM block of the PU. Specifically, the block $\widetilde{\mathbf{z}}_2(n) \in \mathbb{C}^P$, transmitted by the STx during the nth PU symbol period, is composed of two summands $\widetilde{\mathbf{z}}_2(n) = \widetilde{\mathbf{z}}_{2,\text{I}}(n) + \widetilde{\mathbf{z}}_{2,\text{II}}(n)$: the former one $\widetilde{\mathbf{z}}_{2,\text{I}}(n)$ conveys the symbols $\mathbf{x}_{\text{SU,I}}(n) \triangleq [x_{\text{SU}}^{(0)}(n), x_{\text{SU}}^{(1)}(n), \ldots, x_{\text{SU}}^{(N-1)}(n)]^{\text{T}} \in \mathbb{C}^N$ to be transmitted over the Q used subcarriers of the PU, whereas the latter one $\widetilde{\mathbf{z}}_{2,\text{II}}(n)$ is a linear transformation of the symbols $\mathbf{x}_{\text{SU,II}}(n) \triangleq [x_{\text{SU}}^{(N)}(n), x_{\text{SU}}^{(N+1)}(n), \ldots, x_{\text{SU}}^{(N+M_{\text{vc}}-1)}(n)]^{\text{T}} \in \mathbb{C}^{M_{\text{vc}}}$ to be sent over the M_{vc} VCs of the PU. We note that $\mathbf{x}_{\text{SU}}(n) = [\mathbf{x}_{\text{SU,I}}^{\text{T}}(n), \mathbf{x}_{\text{SU,II}}^{\text{T}}(n)]^{\text{T}}$.

The first summand $\widetilde{\mathbf{z}}_{2,\text{I}}(n) \triangleq [\widetilde{z}_{2,\text{I}}^{(0)}(n), \widetilde{z}_{2,\text{I}}^{(1)}(n), \ldots, \widetilde{z}_{2,\text{I}}^{(P-1)}(n)]^{\text{T}} \in \mathbb{C}^P$ is obtained by performing a linear transformation of the received block $\widetilde{\mathbf{y}}_2(n)$ through the Toeplitz lower-triangular matrix

$$\widetilde{\mathbf{F}}(n) \triangleq \sum_{p=0}^{L_{\text{SU}}} \widetilde{f}^{(p)}(n)\, \mathbf{S}_{\text{f}}^{p} \in \mathbb{C}^{P \times P}\,, \quad \text{with } L_{\text{SU}} < M \tag{6}$$

that is, $\widetilde{\mathbf{z}}_{2,\text{I}}(n) = \widetilde{\mathbf{F}}(n)\, \widetilde{\mathbf{y}}_2(n)$, where $\{\widetilde{f}^{(p)}(n)\}_{p=0}^{L_{\text{SU}}}$ piggybacks the symbols in $\mathbf{x}_{\text{SU,I}}(n)$. We note that $\widetilde{\mathbf{z}}_{2,\text{I}}(n)$ depends on the received signal $\widetilde{\mathbf{y}}_2(n)$ and, thus, it must be computed in *real-time*. In this regard, it is noteworthy that, for each $n \in \mathbb{Z}$, the block $\widetilde{\mathbf{z}}_{2,\text{I}}(n)$ can be interpreted as the output of a discrete-time causal LTI filter having $\widetilde{f}^{(p)}(n)$ and $\widetilde{y}_2^{(p)}(n)$ as impulse response and input signal, respectively, i.e.,

$$\widetilde{z}_{2,\text{I}}^{(p)}(n) = \sum_{\ell=0}^{p} \widetilde{f}^{(p-\ell)}(n)\, \widetilde{y}_2^{(\ell)}(n)\,, \quad \text{for } p \in \mathcal{P} \tag{7}$$

supposing that $\widetilde{f}^{(\ell)}(n) = 0$ for $\ell < 0$. The functional dependence of the matrix $\widetilde{\mathbf{F}}(n)$ on the symbol subvector $\mathbf{x}_{\text{SU,I}}(n)$ is much easier to explain in the frequency-domain. For each $n \in \mathbb{Z}$, let $\mathbf{f}(n) \triangleq [F^{(n)}(0), F^{(n)}(1), \ldots, F^{(n)}(M-1)]^{\text{T}} \in \mathbb{C}^M$, with

$$F^{(n)}(m) \triangleq \sum_{\ell=0}^{L_{\text{SU}}} \widetilde{f}^{(\ell)}(n)\, e^{-j\frac{2\pi}{M}\ell m}\,, \quad \text{for } m \in \mathcal{M} \tag{8}$$

being the M-point DFT of $\mathbf{J}\,\widetilde{\mathbf{f}}(n)$, where $\mathbf{J} \triangleq [\mathbf{I}_{L_{\text{SU}}+1}, \mathbf{O}_{(M-L_{\text{SU}}-1)\times(L_{\text{SU}}+1)}^{\text{T}}]^{\text{T}} \in \mathbb{R}^{M\times(L_{\text{SU}}+1)}$ is a zero-padding matrix and $\widetilde{\mathbf{f}}(n) \triangleq [\widetilde{f}^{(0)}(n), \widetilde{f}^{(1)}(n), \ldots, \widetilde{f}^{(L_{\text{SU}})}(n)]^{\text{T}} \in \mathbb{C}^{L_{\text{SU}}+1}$ completely describes the matrix $\widetilde{\mathbf{F}}(n)$ given by (6). In our scheme, we impose that $F^{(m)}(n) = \boldsymbol{\alpha}_m^{\text{H}}\, \mathbf{x}_{\text{SU,I}}(n)$ is a linear combination of the SU symbols, with $\boldsymbol{\alpha}_m \triangleq [\alpha_{m,0}, \alpha_{m,1}, \ldots, \alpha_{m,N-1}]^{\text{T}} \in \mathbb{C}^N$. In this case, it

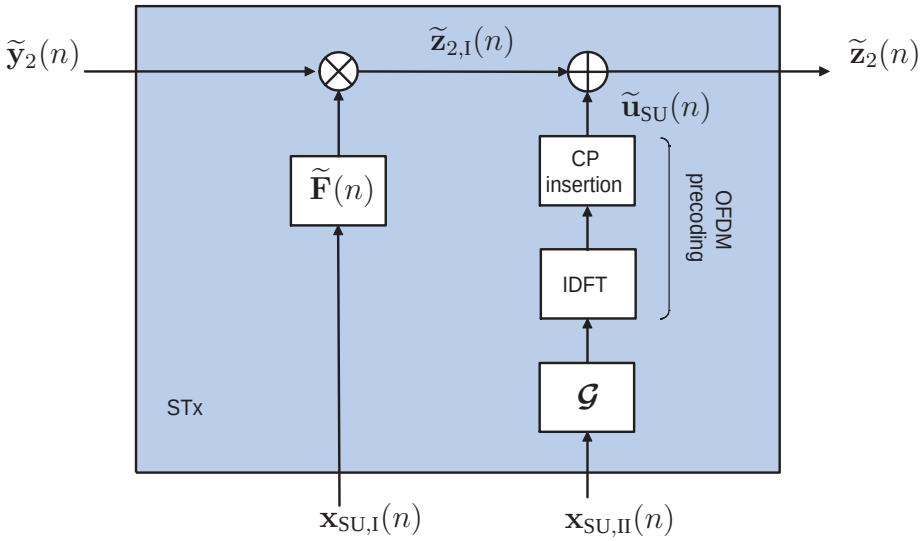

Figure 2. Baseband processing carried out at the secondary user transceiver.

results that $\mathbf{f}(n) = \boldsymbol{\mathcal{A}}\,\mathbf{x}_{\mathrm{SU,I}}(n)$, where $\boldsymbol{\mathcal{A}} \triangleq [\boldsymbol{\alpha}_0, \boldsymbol{\alpha}_1, \ldots, \boldsymbol{\alpha}_{M-1}]^{\mathrm{H}} \in \mathbb{C}^{M\times N}$ is a *frequency-domain precoding matrix* of the SU symbols. In order to ensure that $\mathbf{f}(n) = \mathbf{0}_M$ iff $\mathbf{x}_{\mathrm{SU,I}}(n) = \mathbf{0}_N$, the matrix $\boldsymbol{\mathcal{A}}$ must be full-column rank, i.e., rank$(\boldsymbol{\mathcal{A}}) = N$.

At this point, let us focus on the second summand $\widetilde{\mathbf{z}}_{2,\mathrm{II}}(n) \in \mathbb{C}^P$. Such a vector does not depend on the received data $\widetilde{\mathbf{y}}_2(n)$ and, hence, it is already available at the beginning of the time interval $[nT_{\mathrm{PU}}, (n+1)T_{\mathrm{PU}})$. In our scheme, it is generated as $\widetilde{\mathbf{z}}_{2,\mathrm{II}}(n) \equiv \widetilde{\mathbf{u}}_{\mathrm{SU}}(n) \triangleq \mathbf{T}_{\mathrm{cp}}\,\mathbf{W}_{\mathrm{IDFT}}\,\boldsymbol{\mathcal{G}}\,\mathbf{x}_{\mathrm{SU,II}}(n)$, where $\boldsymbol{\mathcal{G}} \triangleq [\boldsymbol{\gamma}_0, \boldsymbol{\gamma}_1, \ldots, \boldsymbol{\gamma}_{M-1}]^{\mathrm{H}} \in \mathbb{C}^{M\times M_{\mathrm{vc}}}$ is *another* frequency-domain precoding matrix of the SU symbols, with $\boldsymbol{\gamma}_m \in \mathbb{C}^{M_{\mathrm{vc}}}$, whose choice will be clear in Subsection II-E and Section IV.[8] Therefore, the overall time-domain data block transmitted by the STx is given by

$$\widetilde{\mathbf{z}}_2(n) = \widetilde{\mathbf{F}}(n)\,\widetilde{\mathbf{y}}_2(n) + \widetilde{\mathbf{u}}_{\mathrm{SU}}(n) \tag{9}$$

whose entries are subject to D/A plus RF conversion for transmission over the wireless channel. The main signal processing operations carried out by the STx are depicted in Fig. 2. Strictly speaking, the STx acts as a full-duplex AF relay, which linearly processes the received data $\widetilde{\mathbf{y}}_2(n)$ through an own information-bearing matrix $\widetilde{\mathbf{F}}(n)$, by also adding the term $\widetilde{\mathbf{u}}_{\mathrm{SU}}(n)$.

Implementation of the convolution formula (7) requires the synthesis of the time-domain vector

[8]For each $m \in \mathcal{M}$, the weight vectors $\boldsymbol{\alpha}_m$ and $\boldsymbol{\gamma}_m$ might change from one symbol to another. For the sake of simplicity, we will not explicitly indicate the dependence of $\boldsymbol{\mathcal{A}}$ and $\boldsymbol{\mathcal{G}}$ on the PU symbol period.

$\widetilde{\mathbf{f}}(n)$. The relationship between $\widetilde{\mathbf{f}}(n)$ and its frequency-domain counterpart $\mathbf{f}(n)$ is given by

$$\sqrt{M}\,\mathbf{W}_{\text{DFT}}\,\mathbf{J}\,\widetilde{\mathbf{f}}(n) = \mathbf{f}(n) \tag{10}$$

with $\mathbf{W}_{\text{DFT}} \triangleq \mathbf{W}_{\text{IDFT}}^{-1} = \mathbf{W}_{\text{IDFT}}^{\text{H}}$ defining the unitary symmetric DFT matrix [22].

Lemma 1: The system of linear equations (10) is consistent (i.e., it admits at least one solution) iff $\mathbf{f}(n) = \mathbf{\Pi}_{\text{IDFT}}\,\mathbf{r}(n)$, where the columns of $\mathbf{\Pi}_{\text{IDFT}} \in \mathbb{C}^{M\times(L_{\text{SU}}+1)}$ form a basis for the null space of $\overline{\mathbf{W}}_{\text{IDFT}}$, i.e., $\overline{\mathbf{W}}_{\text{IDFT}}\,\mathbf{\Pi}_{\text{IDFT}} = \mathbf{O}_{(M-L_{\text{SU}}-1)\times(L_{\text{SU}}+1)}$,[9] with $\overline{\mathbf{W}}_{\text{IDFT}} \in \mathbb{C}^{(M-L_{\text{SU}}-1)\times M}$ obtained from $\mathbf{W}_{\text{IDFT}}$ by picking its last $M - L_{\text{SU}} - 1$ rows, and $\mathbf{r}(n) \in \mathbb{C}^{L_{\text{SU}}+1}$ is an arbitrary vector.

Proof: System (10) is consistent [19] iff $(\sqrt{M}\,\mathbf{W}_{\text{DFT}}\,\mathbf{J})\,(\sqrt{M}\,\mathbf{W}_{\text{DFT}}\,\mathbf{J})^{-}\,\mathbf{f}(n) = \mathbf{f}(n)$. Since $(\sqrt{M}\,\mathbf{W}_{\text{DFT}}\,\mathbf{J})^{-} = \mathbf{J}^{-}\,\mathbf{W}_{\text{IDFT}}/\sqrt{M}$, with $\mathbf{J}^{-} = \mathbf{J}^{\text{T}}$, the previous equation can be equivalently written after straightforward algebraic manipulations as $(\mathbf{I}_M - \mathbf{J}\,\mathbf{J}^{\text{T}})\,\mathbf{W}_{\text{IDFT}}\,\mathbf{f}(n) = \mathbf{0}_M$ which, accounting for the structure of $\mathbf{J}$ and partitioning $\mathbf{W}_{\text{IDFT}}$ accordingly, leads to the homogeneous system of linear equations $\overline{\mathbf{W}}_{\text{IDFT}}\,\mathbf{f}(n) = \mathbf{0}_{M-L_{\text{SU}}-1}$. Hence, system (10) is consistent iff $\mathbf{f}(n)$ belongs to the null space of $\overline{\mathbf{W}}_{\text{IDFT}}$. The proof ends by observing that $\overline{\mathbf{W}}_{\text{IDFT}}$ is full-row rank, i.e., $\text{rank}(\overline{\mathbf{W}}_{\text{IDFT}}) = M - L_{\text{SU}} - 1$, and, thus, the dimension of its null space (i.e., its nullity) is equal to $M - \text{rank}(\overline{\mathbf{W}}_{\text{IDFT}}) = L_{\text{SU}} + 1$. ■

As an immediate consequence of Lemma 1, one has that the precoding matrix $\boldsymbol{\mathcal{A}}$ cannot be completely arbitrary but, instead, it must obey $\boldsymbol{\mathcal{A}} = \mathbf{\Pi}_{\text{IDFT}}\,\boldsymbol{\mathcal{B}}$, with $\boldsymbol{\mathcal{B}} \in \mathbb{C}^{(L_{\text{SU}}+1)\times N}$. It is important to note that, in this case, the rank condition $\text{rank}(\boldsymbol{\mathcal{A}}) = N$ mandates $\text{rank}(\mathbf{\Pi}_{\text{IDFT}}\,\boldsymbol{\mathcal{B}}) = N$, which happens iff $\text{rank}(\boldsymbol{\mathcal{B}}) = N \leq L_{\text{SU}} + 1$,[10] i.e., the length of the vector $\mathbf{x}_{\text{SU,I}}(n)$ cannot be greater than the filter length $L_{\text{SU}} + 1$. In this case, the *minimal-norm* solution of (10) reads as

$$\widetilde{\mathbf{f}}(n) = (\sqrt{M}\,\mathbf{W}_{\text{DFT}}\,\mathbf{J})^{\dagger}\,\mathbf{f}(n) = \frac{1}{\sqrt{M}}\,\mathbf{J}^{\text{T}}\,\mathbf{W}_{\text{IDFT}}\,\mathbf{\Pi}_{\text{IDFT}}\,\boldsymbol{\mathcal{B}}\,\mathbf{x}_{\text{SU,I}}(n)\,. \tag{11}$$

The choice of $\boldsymbol{\mathcal{B}}$ may depend on the available CSI at the STx and will be discussed in Subsection II-E and Section IV.

As a final remark, the (linear) convolution (7) can be directly calculated in real-time without inherent latency: indeed, if computations were instantaneous, each sample of the received signal would yield a corresponding output to be transmitted by the STx. The actual latency of the direct convolution (7) results from the time necessary to compute each output sample. We will see in

[9]It can be assumed, without loss of generality, that $\mathbf{\Pi}_{\text{IDFT}}$ is semi-unitary i.e., $\mathbf{\Pi}_{\text{IDFT}}^{\text{H}}\,\mathbf{\Pi}_{\text{IDFT}} = \mathbf{I}_{L_{\text{SU}}+1}$.

[10]It results [20] that $\text{rank}(\boldsymbol{\mathcal{B}}) \leq \text{rank}(\mathbf{\Pi}_{\text{IDFT}}\,\boldsymbol{\mathcal{B}}) \leq \min[L_{\text{SU}} + 1, \text{rank}(\boldsymbol{\mathcal{B}})]$.

Subsections II-D and II-E that, due to other constraints, the filter order $L_{\rm SU}$ has to be smaller than $L_{\rm cp}$. The computation time is shorter than the sampling period T_c and, thus, the latency can be assumed to be equal to one sample only. Even though the computational cost of (7) increases linearly with the filter order, with respect to frequency-domain block convolution techniques based on the fast Fourier transform (FFT),[11] the price to pay in terms of computational complexity is negligible when $L_{\rm SU} < L_{\rm cp} \ll M$.

D. Signal received and processed by the PRx

Let $\widetilde{\mathbf{y}}_3(n) \in \mathbb{C}^P$ gather the baseband-equivalent samples received by the PRx within the nth PU symbol period. Accounting for (3) and (9), one gets

$$\begin{aligned}\widetilde{\mathbf{y}}_3(n) &= \widetilde{\mathbf{H}}_{13}^{(0)}\,\widetilde{\mathbf{u}}_{\rm PU}(n) + \widetilde{\mathbf{H}}_{13}^{(1)}\,\widetilde{\mathbf{u}}_{\rm PU}(n-1) + \widetilde{\mathbf{H}}_{23}^{(0)}\,\widetilde{\mathbf{z}}_2(n) + \widetilde{\mathbf{H}}_{23}^{(1)}\,\widetilde{\mathbf{z}}_2(n-1) + \widetilde{\mathbf{v}}_3(n)\\ &= \left[\widetilde{\mathbf{H}}_{13}^{(0)} + \widetilde{\mathbf{H}}_{23}^{(0)}\,\widetilde{\mathbf{F}}(n)\,\widetilde{\mathbf{H}}_{12}^{(0)}\right]\widetilde{\mathbf{u}}_{\rm PU}(n) + \left[\widetilde{\mathbf{H}}_{13}^{(1)} + \widetilde{\mathbf{H}}_{23}^{(0)}\,\widetilde{\mathbf{F}}(n)\,\widetilde{\mathbf{H}}_{12}^{(1)} + \widetilde{\mathbf{H}}_{23}^{(1)}\,\widetilde{\mathbf{F}}(n-1)\,\widetilde{\mathbf{H}}_{12}^{(0)}\right]\widetilde{\mathbf{u}}_{\rm PU}(n-1)\\ &\quad + \widetilde{\mathbf{H}}_{23}^{(1)}\,\widetilde{\mathbf{F}}(n-1)\,\widetilde{\mathbf{H}}_{12}^{(1)}\,\widetilde{\mathbf{u}}_{\rm PU}(n-2) + \widetilde{\mathbf{H}}_{23}^{(0)}\,\widetilde{\mathbf{u}}_{\rm SU}(n) + \widetilde{\mathbf{H}}_{23}^{(1)}\,\widetilde{\mathbf{u}}_{\rm SU}(n-1)\\ &\quad + \widetilde{\mathbf{H}}_{23}^{(0)}\,\widetilde{\mathbf{F}}(n)\,\widetilde{\mathbf{v}}_2(n) + \widetilde{\mathbf{H}}_{23}^{(1)}\,\widetilde{\mathbf{F}}(n-1)\,\widetilde{\mathbf{v}}_2(n-1) + \widetilde{\mathbf{v}}_3(n) \quad (12)\end{aligned}$$

where $\{\widetilde{\mathbf{H}}_{13}^{(0)}, \widetilde{\mathbf{H}}_{13}^{(1)}\}$ and $\{\widetilde{\mathbf{H}}_{23}^{(0)}, \widetilde{\mathbf{H}}_{23}^{(1)}\}$ can be obtained from (4) and (5) by replacing $\{L_{12}, \widetilde{h}_{12}(\ell), \theta_{12}\}$ with $\{L_{13}, \widetilde{h}_{13}(\ell), \theta_{13}\}$ and $\{L_{23}, \widetilde{h}_{23}(\ell), \theta_{23}\}$, respectively, and we remember that $\widetilde{\mathbf{v}}_3(n)$ accounts for noise.

The product of any lower (upper) triangular Toeplitz matrices is a lower (upper) triangular Toeplitz matrix, too [20]. Indeed, it is directly verified that, if the following inequality

$$L_{12} + L_{\rm SU} + L_{23} + \theta_{12} + \theta_{23} \leq P - 1 \quad (13)$$

holds, the product $\widetilde{\mathbf{H}}_{23}^{(0)}\,\widetilde{\mathbf{F}}(n)\,\widetilde{\mathbf{H}}_{12}^{(0)}$ is a lower-triangular Toeplitz matrix having as first column $[\mathbf{0}_{\theta_{12}+\theta_{23}}^{\rm T}, \widetilde{\mathbf{h}}_{123}^{\rm T}(n), \mathbf{0}_{P-L_{12}-L_{\rm SU}-L_{23}-\theta_{12}-\theta_{23}-1}^{\rm T}]^{\rm T}$, where the vector $\widetilde{\mathbf{h}}_{123} \in \mathbb{C}^{L_{12}+L_{\rm SU}+L_{23}+1}$ collects the samples of the (linear) convolution among $\{\widetilde{h}_{12}(\ell)\}_{\ell=0}^{L_{12}}$, $\{\widetilde{f}^{(\ell)}(n)\}_{\ell=0}^{L_{\rm SU}}$, and $\{\widetilde{h}_{23}(\ell)\}_{\ell=0}^{L_{23}}$. Moreover, one has $\widetilde{\mathbf{H}}_{23}^{(1)}\,\widetilde{\mathbf{F}}(n-1)\,\widetilde{\mathbf{H}}_{12}^{(1)} = \mathbf{O}_{P\times P}$, provided that (13) is fulfilled. On the other hand, it is verified by direct inspection that: (i) only the first $L_{12} + L_{\rm SU} + L_{23} + \theta_{12} + \theta_{23}$ rows of $\widetilde{\mathbf{H}}_{23}^{(0)}\,\widetilde{\mathbf{F}}(n)\,\widetilde{\mathbf{H}}_{12}^{(1)}$ might not be zero; (ii) the last $P - L_{i3} - \theta_{i3}$ rows of the matrix $\widetilde{\mathbf{H}}_{i3}^{(1)}$ are identically zero, for

[11] Computationally efficient FFT-based methods cannot be used for evaluating the linear convolution (7) since they have an inherent input-to-output latency equal to the length P of the block, i.e., one symbol period $T_{\rm PU}$: indeed, the input block $\widetilde{\mathbf{y}}_2(n)$ must be fully available in order to start computing the the samples of the output block $\widetilde{\mathbf{z}}_{2,\rm I}(n)$.

$i \in \{1,2\}$; (iii) the nonzero entries of $\widetilde{\mathbf{H}}_{23}^{(1)}\,\widetilde{\mathbf{F}}(n-1)\,\widetilde{\mathbf{H}}_{12}^{(0)}$ and $\widetilde{\mathbf{H}}_{23}^{(1)}\,\widetilde{\mathbf{F}}(n-1)\,\widetilde{\mathbf{v}}_2(n-1)$ are located within their first $L_{23}+\theta_{23}$ rows. Therefore, if the CP is designed such that

$$L_{\text{cp}} \geq \max\left(L_{12}+L_{\text{SU}}+L_{23}+\theta_{12}+\theta_{23}, L_{13}+\theta_{13}\right) \tag{14}$$

the IBI contribution in (12) can be completely discarded by dropping the first L_{cp} components of $\widetilde{\mathbf{y}}_3(n)$. In other words, the convolutive process carried out by the STx may increase the frequency selectivity of the end-to-end PU channel. This drawback can be overcome by increasing the CP length as in (14), which leads to an inherent reduction of the transmission data rate of the PU system when $L_{12}+L_{\text{SU}}+L_{23}+\theta_{12}+\theta_{23} > L_{13}+\theta_{13}$. However, such a (possible) loss turns out to be negligible if the number M of subcarriers is significantly greater than L_{cp}. Most important, we show in Section III that, if the legacy system is designed to fulfil (14), it might even achieve a significant performance gain. Moreover, assumption (14) requires only upper bounds (rather than the exact knowledge) on the channel orders and TOs. In general, depending on the transmitted signal parameters (carrier frequency and bandwidth) and environment (indoor or outdoor), the maximum channel multipath spread is known and the TOs are confined to a small uncertainty interval, whose support can be typically predicted.

CP removal is accomplished by defining the matrix $\mathbf{R}_{\text{cp}} \triangleq [\mathbf{O}_{M\times L_{\text{cp}}}, \mathbf{I}_M] \in \mathbb{R}^{M\times P}$ and forming the product $\mathbf{R}_{\text{cp}}\,\widetilde{\mathbf{y}}_3(n)$. If (11) and (14) hold, after discarding the CP and performing M-point DFT, the received signal over all the subcarriers at the PRx can be expressed as follows

$$\mathbf{y}_{\text{PU}}(n) \equiv \mathbf{y}_3(n) \triangleq \mathbf{W}_{\text{DFT}}\,\mathbf{R}_{\text{cp}}\,\widetilde{\mathbf{y}}_3(n) = \boldsymbol{\mathcal{H}}_{\text{PU}}(n)\,\boldsymbol{\Theta}\,\mathbf{x}_{\text{PU}}(n) + \mathbf{v}_{\text{PU}}(n) \tag{15}$$

where $\boldsymbol{\mathcal{H}}_{\text{PU}}(n) \triangleq \boldsymbol{\mathcal{H}}_{13} + \boldsymbol{\mathcal{H}}_{23}\,\boldsymbol{\mathcal{F}}(n)\,\boldsymbol{\mathcal{H}}_{12} \in \mathbb{C}^{M\times M}$ is a diagonal matrix whose mth diagonal entry is given by

$$H_{\text{PU}}(m) \triangleq H_{13}(m) + H_{12}(m)\,H_{23}(m)\,F^{(n)}(m)\,, \quad \text{with } m \in \mathcal{M} \tag{16}$$

with $F^{(n)}(m) = \{\mathbf{f}(n)\}_m = \{\boldsymbol{\Pi}_{\text{IDFT}}\,\boldsymbol{\mathcal{B}}\,\mathbf{x}_{\text{SU,I}}(n)\}_m$, and

$$\mathbf{v}_{\text{PU}}(n) \triangleq \mathbf{W}_{\text{DFT}}\,\mathbf{R}_{\text{cp}}\,\widetilde{\mathbf{H}}_{23}^{(0)}\,\widetilde{\mathbf{F}}(n)\,\widetilde{\mathbf{v}}_2(n) + \boldsymbol{\mathcal{H}}_{23}\,\boldsymbol{\mathcal{G}}\,\mathbf{x}_{\text{SU,II}}(n) + \mathbf{v}_3(n) \in \mathbb{C}^M \tag{17}$$

represents the *equivalent noise* vector at the PRx, the matrices $\boldsymbol{\mathcal{H}}_{13}$ and $\boldsymbol{\mathcal{H}}_{23}$ have been defined in (1), whereas $\boldsymbol{\mathcal{F}}(n) \triangleq \text{diag}[\mathbf{f}(n)] = \text{diag}[\boldsymbol{\Pi}_{\text{IDFT}}\,\boldsymbol{\mathcal{B}}\,\mathbf{x}_{\text{SU,I}}(n)] \in \mathbb{C}^{M\times M}$ collects the M-point DFT samples (8), and $\mathbf{v}_j(n) \triangleq [v_j^{(0)}(n), v_j^{(1)}(n), \ldots, v_j^{(M-1)}(n)]^{\text{T}} = \mathbf{W}_{\text{DFT}}\,\mathbf{R}_{\text{cp}}\,\widetilde{\mathbf{v}}_j(n) \in \mathbb{C}^M$, for $j \in \{2,3\}$. It is apparent that the overall PU channel matrix $\boldsymbol{\mathcal{H}}_{\text{PU}}(n)$ incorporates the contribution

of the SU symbol block $\mathbf{x}_{\text{SU}}(n)$. The entries of $\boldsymbol{\mathcal{H}}_{\text{PU}}(n)$ can be estimated at the PRx using training symbols transmitted by the PTx and, thus, knowledge of $\boldsymbol{\mathcal{F}}(n)$ is not required at the PRx.[12]

E. Signal received and processed by the SRx

Similarly to (12), the baseband-equivalent received data vector by the SRx within the nth PU symbol period can be expressed as

$$\widetilde{\mathbf{y}}_4(n) = \widetilde{\mathbf{H}}_{14}^{(0)}\,\widetilde{\mathbf{u}}_{\text{PU}}(n) + \widetilde{\mathbf{H}}_{14}^{(1)}\,\widetilde{\mathbf{u}}_{\text{PU}}(n-1) + \widetilde{\mathbf{H}}_{24}^{(0)}\,\widetilde{\mathbf{z}}_2(n) + \widetilde{\mathbf{H}}_{24}^{(1)}\,\widetilde{\mathbf{z}}_2(n-1) + \widetilde{\mathbf{v}}_4(n) \tag{18}$$

where $\{\widetilde{\mathbf{H}}_{14}^{(0)}, \widetilde{\mathbf{H}}_{14}^{(1)}\}$ and $\{\widetilde{\mathbf{H}}_{24}^{(0)}, \widetilde{\mathbf{H}}_{24}^{(1)}\}$ can be obtained from (4) and (5) by replacing $\{L_{12}, \widetilde{h}_{12}(\ell), \theta_{12}\}$ with $\{L_{14}, \widetilde{h}_{14}(\ell), \theta_{14}\}$ and $\{L_{24}, \widetilde{h}_{24}(\ell), \theta_{24}\}$, respectively, and we remember that $\widetilde{\mathbf{v}}_4(n)$ is the noise vector. Paralleling the same arguments of Subsection II-D, it can be shown that, if $L_{12} + L_{\text{SU}} + L_{24} + \theta_{12} + \theta_{24} \leq P - 1$ and[13]

$$L_{\text{cp}} \geq \max\left(L_{12} + L_{\text{SU}} + L_{24} + \theta_{12} + \theta_{24}, L_{14} + \theta_{14}\right) \tag{19}$$

after discarding the CP and performing M-point DFT, the frequency-domain signal received at the SRx can be written as

$$\mathbf{y}_{\text{SU}}(n) \equiv \mathbf{y}_4(n) \triangleq \mathbf{W}_{\text{DFT}}\,\mathbf{R}_{\text{cp}}\,\widetilde{\mathbf{y}}_4(n) = \boldsymbol{\mathcal{H}}_{\text{SU}}(n)\,\boldsymbol{\Delta}\,\mathbf{x}_{\text{SU}}(n) + \mathbf{v}_{\text{SU}}(n) \tag{20}$$

where $\boldsymbol{\mathcal{H}}_{\text{SU}}(n) \triangleq [\mathbf{H}_{\text{SU}}(n), \boldsymbol{\mathcal{H}}_{24}] \in \mathbb{C}^{M\times 2M}$, $\mathbf{H}_{\text{SU}}(n) \triangleq \boldsymbol{\mathcal{H}}_{24}\,[\boldsymbol{\mathcal{H}}_{12}\,\mathbf{X}_{\text{PU}}(n) + \mathbf{V}_2(n)] \in \mathbb{C}^{M\times M}$, $\boldsymbol{\Delta} \triangleq \text{diag}(\boldsymbol{\Pi}_{\text{IDFT}}\,\boldsymbol{\mathcal{B}}, \boldsymbol{\mathcal{G}}) \in \mathbb{C}^{2M\times(N+M_{\text{vc}})}$ represents the *overall* frequency-domain precoding matrix of the SU, and $\mathbf{v}_{\text{SU}}(n) \triangleq \boldsymbol{\mathcal{H}}_{14}\,\boldsymbol{\Theta}\,\mathbf{x}_{\text{PU}}(n) + \mathbf{v}_4(n) \in \mathbb{C}^M$ denotes the *equivalent noise* term at the SRx. Additionally, $\mathbf{X}_{\text{PU}}(n) \triangleq \text{diag}[\boldsymbol{\Theta}\,\mathbf{x}_{\text{PU}}(n)] \in \mathbb{C}^{M\times M}$, $\mathbf{V}_2(n) \triangleq \text{diag}[\mathbf{v}_2(n)] \in \mathbb{C}^{M\times M}$, $\mathbf{v}_4(n) \triangleq \mathbf{W}_{\text{DFT}}\,\mathbf{R}_{\text{cp}}\,\widetilde{\mathbf{v}}_4(n) \in \mathbb{C}^M$, and the diagonal channel matrices $\boldsymbol{\mathcal{H}}_{14}$ and $\boldsymbol{\mathcal{H}}_{24}$ have been defined in (1). In writing (20), we have replaced the noise vector $\widetilde{\mathbf{v}}_2(n)$ with $\hat{\mathbf{v}}_2(n) \triangleq \mathbf{T}_{\text{cp}}\,\mathbf{v}_2(n)$: they are both ZMCSCG random vectors with correlation matrix $\mathsf{E}[\widetilde{\mathbf{v}}_2(n)\,\widetilde{\mathbf{v}}_2^{\text{H}}(n)] = \sigma_{v_2}^2\,\mathbf{I}_P$ and $\mathsf{E}[\hat{\mathbf{v}}_2(n)\,\hat{\mathbf{v}}_2(n)^{\text{H}}] = \sigma_{v_2}^2\,\mathbf{T}_{\text{cp}}\,\mathbf{T}_{\text{cp}}^{\text{T}}$, respectively. For sufficiently large values of M, the matrices $\mathbf{I}_P$ and $\mathbf{T}_{\text{cp}}\,\mathbf{T}_{\text{cp}}^{\text{T}}$ are asymptotically equivalent in weak norm [26]. Therefore, in the large M limit,

[12]The channel estimation error can be made negligible, for intermediate-to-high SNRs, by using a number of training symbols that is not smaller than L_{cp} and by carefully designing the PU training sequence [23].

[13]To suppress only its own IBI represented by $\widetilde{\mathbf{u}}_{\text{SU}}(n-1)$, the SRx could even discard a portion of the received data smaller than L_{cp}, thus accepting the IBI of the PU transmission due to $\widetilde{\mathbf{u}}_{\text{PU}}(n-1)$. However, in this case, more complex receiving structures would be required to reliably estimate the desired symbol block $\mathbf{x}_{\text{SU}}(n)$ [24], [25].

the random vectors $\widetilde{\mathbf{v}}_2(n)$ and $\hat{\mathbf{v}}_2(n)$ have the same distribution. Moreover, it is noteworthy that the channel matrix $\mathbf{H}_{\text{SU}}(n)$ is a diagonal matrix, whose mth diagonal entry is given by

$$H_{\text{SU}}^{(n)}(m) = H_{24}(m)\,[H_{12}(m)\,x_{\text{PU}}^{(m)}(n)\,\beta_m + v_2^{(m)}(n)] \tag{21}$$

where $\beta_m = 0$ if $m \in \mathcal{I}_{\text{PU,vc}}$, whereas $\beta_m = 1$ if $m \in \mathcal{I}_{\text{PU,uc}} \triangleq \{0, 1, \ldots, M-1\} - \mathcal{I}_{\text{PU,vc}}$, which represents the set of PU used subcarriers. The "composite" matrix $\boldsymbol{\mathcal{H}}_{\text{SU}}(n)$ in (20) can be reliably estimated at the SRx using training symbols transmitted by the STx (footnote 12 also applies in this case with obvious modifications). Signal models (15) and (20) hold if the CP of the PU system is designed to satisfy both inequalities (14) and (19). Such an assumption is quite reasonable when the STx is very close to the PTx, which is the network scenario where our proposed scheme ensures a significant performance gain for the PU system (see Section III).

Some preliminary comments are now in order regarding the choice of the precoding matrices $\boldsymbol{\mathcal{A}} = \boldsymbol{\Pi}_{\text{IDFT}}\,\boldsymbol{\mathcal{B}}$ and $\boldsymbol{\mathcal{G}}$. Since $H_{\text{SU}}^{(n)}(m) = H_{24}(m)\,v_2^{(m)}(n)$ for $m \in \mathcal{I}_{\text{PU,vc}}$, over the PU VCs, the time-domain convolution (7) leads to a multiplicative superposition of the SU symbols on the noise samples $\{v_2^{(m)}(n)\}_{m\in\mathcal{I}_{\text{PU,vc}}}$: it is intuitive that, from the SU viewpoint, such a strategy is detrimental for vanishingly small noise variances. Therefore, any reasonable optimization criterion of the SU precoder will impose that $\boldsymbol{\alpha}_{q_0} = \boldsymbol{\alpha}_{q_1} = \cdots = \boldsymbol{\alpha}_{q_{M_{\text{vc}}-1}} = \mathbf{0}_N$. Since the mth row of $\boldsymbol{\mathcal{A}}$ is given by $\boldsymbol{\alpha}_m^{\text{H}} = [\boldsymbol{\pi}_{\text{IDFT}}^{(m)}]^{\text{H}}\,\boldsymbol{\mathcal{B}}$, where the conjugate transpose of $\boldsymbol{\pi}_{\text{IDFT}}^{(m)} \in \mathbb{C}^{L_{\text{SU}}+1}$ is the mth row of $\boldsymbol{\Pi}_{\text{IDFT}}$, for $m \in \mathcal{M}$, such a condition is tantamount to the matrix equation $\boldsymbol{\mathcal{B}}^{\text{H}}\,\boldsymbol{\Pi}_{\text{vc}} = \mathbf{O}_{N\times M_{\text{vc}}}$, with $\boldsymbol{\Pi}_{\text{vc}} \triangleq [\boldsymbol{\pi}_{\text{IDFT}}^{(q_0)}, \boldsymbol{\pi}_{\text{IDFT}}^{(q_1)}, \ldots, \boldsymbol{\pi}_{\text{IDFT}}^{(q_{M_{\text{vc}}-1})}] \in \mathbb{C}^{(L_{\text{SU}}+1)\times M_{\text{vc}}}$, whose general solution [19] can be written as

$$\boldsymbol{\mathcal{B}} = \boldsymbol{\Upsilon}_{\text{vc}}\,\boldsymbol{\mathcal{C}} \quad \Rightarrow \quad \boldsymbol{\mathcal{A}} = \boldsymbol{\Pi}_{\text{IDFT}}\,\boldsymbol{\Upsilon}_{\text{vc}}\,\boldsymbol{\mathcal{C}} \tag{22}$$

where the columns of $\boldsymbol{\Upsilon}_{\text{vc}} \in \mathbb{C}^{(L_{\text{SU}}+1)\times(L_{\text{SU}}-R_{\text{vc}}+1)}$ form a basis for the null space of $\boldsymbol{\Pi}_{\text{vc}}^{\text{H}}$, i.e., $\boldsymbol{\Pi}_{\text{vc}}^{\text{H}}\,\boldsymbol{\Upsilon}_{\text{vc}} = \mathbf{O}_{M_{\text{vc}}\times(L_{\text{SU}}-R_{\text{vc}}+1)}$,[14] $\boldsymbol{\mathcal{C}} \in \mathbb{C}^{(L_{\text{SU}}-R_{\text{vc}}+1)\times N}$ is an arbitrary matrix to be designed, and $R_{\text{vc}} \triangleq \text{rank}(\boldsymbol{\Pi}_{\text{vc}}) = \min(L_{\text{SU}}+1, M_{\text{vc}})$. Remembering $\text{rank}(\boldsymbol{\mathcal{B}}) = N \leq L_{\text{SU}}+1$, it follows from (22) that $\text{rank}(\boldsymbol{\Upsilon}_{\text{vc}}\,\boldsymbol{\mathcal{C}}) = N$, which happens iff $\text{rank}(\boldsymbol{\mathcal{C}}) = N \leq L_{\text{SU}} - R_{\text{vc}} + 1$.[15] Factorization (22) further reduces the number N of symbols that the SU can transmit on the PU used subcarriers: in particular, the SU can send information over such subcarriers only if $L_{\text{SU}} + 1 > M_{\text{vc}}$ and, thus, $R_{\text{vc}} = M_{\text{vc}}$. In this setting, to allow the SU to transmit as many symbols as possible, we assume

[14] It can be assumed, without loss of generality, that $\boldsymbol{\Upsilon}_{\text{vc}}$ is semi-unitary i.e., $\boldsymbol{\Upsilon}_{\text{vc}}^{\text{H}}\,\boldsymbol{\Upsilon}_{\text{vc}} = \mathbf{I}_{L_{\text{SU}}-R_{\text{vc}}+1}$.

[15] It results [20] that $\text{rank}(\boldsymbol{\mathcal{C}}) \leq \text{rank}(\boldsymbol{\Upsilon}_{\text{vc}}\,\boldsymbol{\mathcal{C}}) \leq \min[L_{\text{SU}} - R_{\text{vc}} + 1, \text{rank}(\boldsymbol{\mathcal{C}})]$.

hereinafter that $N = L_{\text{SU}} - M_{\text{vc}} + 1$, which implies that $\boldsymbol{\mathcal{C}}$ is square and nonsingular. The design of the matrix $\boldsymbol{\mathcal{C}}$ is discussed in Section IV.

The PU VCs are a precious communication resource for the SU that cannot be wasted. For such a reason, the term $\widetilde{\mathbf{u}}_{\text{SU}}(n)$ in the right-hand side (RHS) of (9) has been introduced aimed at managing the SU transmission over the PU VCs. To this goal, we impose that[16] $\boldsymbol{\gamma}_m = \mathbf{0}_{M_{\text{vc}}}$, $\forall m \in \mathcal{I}_{\text{PU,uc}}$, which leads to the factorization $\boldsymbol{\mathcal{G}} = \boldsymbol{\Xi}\,\boldsymbol{\mathcal{D}}$, where the matrix $\boldsymbol{\Xi} \in \mathbb{R}^{M \times M_{\text{vc}}}$ inserts zero rows in $\boldsymbol{\mathcal{G}}$ over the PU used subcarriers and $\boldsymbol{\mathcal{D}} \triangleq [\boldsymbol{\gamma}_{q_0}, \boldsymbol{\gamma}_{q_1}, \ldots, \boldsymbol{\gamma}_{q_{M_{\text{vc}}-1}}]^{\text{H}} \in \mathbb{C}^{M_{\text{vc}} \times M_{\text{vc}}}$ is an arbitrary matrix, whose choice is deferred to Section IV, which is used to transmit in parallel a linear combination of the entries of the symbol vector $\mathbf{x}_{\text{SU,II}}(n)$ on all the PU VCs.

To limit the average transmit power of the STx (in units of energy per PU symbol), we consider the frequency-domain version of the signal (9) transmitted by the STx, which assumes the expression $\mathbf{z}_2(n) \triangleq \mathbf{W}_{\text{DFT}}\,\mathbf{R}_{\text{cp}}\,\widetilde{\mathbf{z}}_2(n) = \boldsymbol{\mathcal{F}}(n)\,\mathbf{y}_2(n) + \boldsymbol{\mathcal{G}}\,\mathbf{x}_{\text{SU,II}}(n)$, where the vector $\mathbf{y}_2(n) \triangleq \mathbf{W}_{\text{DFT}}\,\mathbf{R}_{\text{cp}}\,\widetilde{\mathbf{y}}_2(n) = \boldsymbol{\mathcal{H}}_{12}\,\boldsymbol{\Theta}\,\mathbf{x}_{\text{PU}}(n) + \mathbf{v}_2(n)$ is the frequency-domain block received by the STx [see (3)]. Power allocation over the different subcarriers is adjusted at the STx according to the constraint $\mathsf{E}\,[\|\mathbf{z}_2(n)\|^2] = \mathsf{P}_{\text{SU}}$, where $\mathsf{P}_{\text{SU}} > 0$ is the SU power budget. Since $\mathsf{E}[|F^{(m)}(n)|^2] = \|\boldsymbol{\alpha}_m\|^2$, $\mathsf{E}[\|\boldsymbol{\mathcal{G}}\,\mathbf{x}_{\text{SU,II}}(n)\|^2] = \sum_{m \in \mathcal{I}_{\text{PU,vc}}} \|\boldsymbol{\gamma}_m\|^2$, and $\mathsf{E}[\mathbf{x}_{\text{SU,II}}(n)\,\mathbf{y}_2^{\text{H}}(n)] = \mathbf{O}_{M_{\text{vc}} \times M}$, such a constraint imposes that

$$(\sigma_{12}^2\,\mathsf{P}_{\text{PU}} + \sigma_{v_2}^2) \sum_{m \in \mathcal{I}_{\text{PU,uc}}} \|\boldsymbol{\alpha}_m\|^2 + \sum_{m \in \mathcal{I}_{\text{PU,vc}}} \|\boldsymbol{\gamma}_m\|^2 = \mathsf{P}_{\text{SU}} \tag{23}$$

where, according to (22), one has $\|\boldsymbol{\alpha}_m\|^2 = \|\boldsymbol{\mathcal{C}}^{\text{H}}\,\boldsymbol{\Upsilon}_{\text{vc}}^{\text{H}}\,\boldsymbol{\pi}_{\text{IDFT}}^{(m)}\|^2$.

III. Worst-case ergodic capacity of the PU

Herein, we show that, under appropriate conditions, the concurrent transmission of the SU can maintain or even improve the performance of the PU. With this goal in mind, we derive the expression of a lower bound on the mutual information of the PU system with CSI at the receiver (CSIR). This expression is used to compute a lower bound on the ergodic channel capacity of the PU, which generalizes and subsumes as a particular case the results reported in [12], [13].[17] Since the detection process at the PRx is carried out on a frame-by-frame basis, we omit the dependence on the frame index n hereinafter.

[16] If the PU does not use VCs, i.e., $M_{\text{vc}} = 0$, then $\boldsymbol{\mathcal{G}} = \mathbf{O}_{M \times M_{\text{vc}}}$ and the second summand in the RHS of (9) disappears.

[17] The upper bound on the PU ergodic capacity reported in [12], [13] can be generalized with similar arguments as well.

With reference to the signal model (15), the computation of a general expression of the mutual information $\mathsf{I}(\mathbf{x}_{\text{PU}}, \mathbf{y}_{\text{PU}} \,|\, \boldsymbol{\mathcal{H}}_{\text{PU}})$ (in bits/s/Hz) between $\mathbf{x}_{\text{PU}}$ and $\mathbf{y}_{\text{PU}}$, given $\boldsymbol{\mathcal{H}}_{\text{PU}}$, is significantly complicated by the fact that $\mathbf{v}_{\text{PU}}$ given by (17) is not a Gaussian random vector. However, a lower bound on $\mathsf{I}(\mathbf{x}_{\text{PU}}, \mathbf{y}_{\text{PU}} \,|\, \boldsymbol{\mathcal{H}}_{\text{PU}})$ can be obtained by observing that the ZMCSCG distribution is the worst-case noise distribution under a variance constraint.[18] First of all, to simplify matters, as already done in (II-E), we replace in (17) the noise vector $\widetilde{\mathbf{v}}_2$ with $\hat{\mathbf{v}}_2 = \mathbf{T}_{\text{cp}}\, \mathbf{v}_2$, which allows one to replace $\mathbf{W}_{\text{DFT}}\, \mathbf{R}_{\text{cp}}\, \widetilde{\mathbf{H}}_{23}^{(0)}\, \widetilde{\mathbf{F}}\, \widetilde{\mathbf{v}}_2$ with $\boldsymbol{\mathcal{H}}_{23}\, \boldsymbol{\mathcal{F}}\, \mathbf{v}_2$. Second, by assuming that $\mathbf{v}_{\text{PU}}$ is a ZMCSCG random vector with (diagonal) correlation matrix

$$\mathbf{R}_{\mathbf{v}_{\text{PU}}} \triangleq \mathsf{E}[\mathbf{v}_{\text{PU}}\, \mathbf{v}_{\text{PU}}^{\text{H}}] = \sigma_{23}^2\, (\sigma_{v_2}^2\, \boldsymbol{\Sigma}_{\mathbf{A}} + \boldsymbol{\Sigma}_{\mathbf{G}}) + \sigma_{v_3}^2\, \mathbf{I}_M \tag{24}$$

where $\boldsymbol{\Sigma}_{\boldsymbol{\mathcal{A}}} \triangleq \text{diag}(\|\boldsymbol{\alpha}_0\|^2, \|\boldsymbol{\alpha}_1\|^2, \ldots, \|\boldsymbol{\alpha}_{M-1}\|^2)$ and $\boldsymbol{\Sigma}_{\boldsymbol{\mathcal{G}}} \triangleq \text{diag}(\|\boldsymbol{\gamma}_0\|^2, \|\boldsymbol{\gamma}_1\|^2, \ldots, \|\boldsymbol{\gamma}_{M-1}\|^2)$, and remembering also that the input distribution maximizing the capacity of the channel in (15) is the ZMCSCG distribution [17], [18], too, that is, $\mathbf{x}_{\text{PU}}$ is a ZMCSCG with correlation matrix $\mathsf{E}[\mathbf{x}_{\text{PU}}\, \mathbf{x}_{\text{PU}}^{\text{H}}] = \mathsf{P}_{\text{PU}}\, \mathbf{I}_Q$, the conditional mutual information $\mathsf{I}(\mathbf{x}_{\text{PU}}, \mathbf{y}_{\text{PU}} \,|\, \boldsymbol{\mathcal{H}}_{\text{PU}})$ under an average transmit power constraint is lower bounded [17], [18] as[19]

$$\mathsf{I}(\mathbf{x}_{\text{PU}}, \mathbf{y}_{\text{PU}} \,|\, \boldsymbol{\mathcal{H}}_{\text{PU}}) \geq \frac{1}{M}\, \log_2 \left[\frac{\det(\mathbf{R}_{\mathbf{v}_{\text{PU}}} + \mathsf{P}_{\text{PU}}\, \boldsymbol{\mathcal{H}}_{\text{PU}}\, \boldsymbol{\Theta}\, \boldsymbol{\Theta}^{\text{T}}\, \boldsymbol{\mathcal{H}}_{\text{PU}}^{*})}{\det(\mathbf{R}_{\mathbf{v}_{\text{PU}}})} \right] \tag{25}$$

where $\mathsf{E}[\|\mathbf{x}_{\text{PU}}\|^2] = Q\, \mathsf{P}_{\text{PU}}$ is the transmit power and the matrix $\mathbf{R}_{\mathbf{v}_{\text{PU}}}$ is nonsingular, i.e., $\det(\mathbf{R}_{\mathbf{v}_{\text{PU}}}) \neq 0$, for SNR values of practical interest.

The ergodic capacity is given by $\mathsf{C}_{\text{PU}} \triangleq \mathsf{E}[\mathsf{I}(\mathbf{x}_{\text{PU}}, \mathbf{y}_{\text{PU}} \,|\, \boldsymbol{\mathcal{H}}_{\text{PU}})]$, where the ensemble average is taken with respect to $\boldsymbol{\mathcal{H}}_{\text{PU}}$. By virtue of (25), it follows that

$$\begin{aligned}
\mathsf{C}_{\text{PU}} \geq \mathsf{C}_{\text{PU,lower}} &\triangleq \frac{1}{M}\, \mathsf{E} \left\{ \log_2 \left[\frac{\det(\mathbf{R}_{\mathbf{v}_{\text{PU}}} + \mathsf{P}_{\text{PU}}\, \boldsymbol{\mathcal{H}}_{\text{PU}}\, \boldsymbol{\Theta}\, \boldsymbol{\Theta}^{\text{T}}\, \boldsymbol{\mathcal{H}}_{\text{PU}}^{*})}{\det(\mathbf{R}_{\mathbf{v}_{\text{PU}}})} \right] \right\} \\
&= \frac{1}{M} \sum_{m=0}^{M-1} \mathsf{E} \left\{ \log_2 \left[1 + \frac{\mathsf{P}_{\text{PU}}\, |H_{\text{PU}}(m)|^2\, \beta_m}{\sigma_{23}^2\, (\sigma_{v_2}^2\, \|\boldsymbol{\alpha}_m\|^2 + \|\boldsymbol{\gamma}_m\|^2) + \sigma_{v_3}^2} \right] \right\} \\
&= \frac{1}{M} \sum_{m \in \mathcal{I}_{\text{PU,uc}}} \mathsf{E} \left[\log_2 \left(1 + \frac{\mathsf{P}_{\text{PU}}\, |H_{\text{PU}}(m)|^2}{\sigma_{23}^2\, \sigma_{v_2}^2\, \|\boldsymbol{\alpha}_m\|^2 + \sigma_{v_3}^2} \right) \right]
\end{aligned} \tag{26}$$

where we have remembered that $\beta_m = 1$ and $\boldsymbol{\gamma}_m = \mathbf{0}_N$ if $m \in \mathcal{I}_{\text{PU,uc}}$, whereas $\beta_m = 0$ otherwise. It is noteworthy that equality in (26) holds when the SU is inactive, i.e., $\boldsymbol{\mathcal{A}} = \boldsymbol{\mathcal{G}} = \mathbf{O}_{M \times N}$:

[18]Given a variance constraint, the Gaussian noise minimizes the capacity of a point-to-point additive noise channel [17], [18], since the Gaussian distribution maximizes the entropy subject to a variance constraint.

[19]The loss in spectral efficiency due to the presence of the CP is neglected throughout our capacity analysis.

indeed, in this case, it results that $\mathbf{v}_{\text{PU}} \equiv \mathbf{v}_3$ is a ZMCSCG random vector with correlation matrix $\mathbf{R}_{\mathbf{v}_{\text{PU}}} = \sigma_{v_3}^2\,\mathbf{I}_M$ and C_{PU} ends up to the ergodic capacity $\mathsf{C}_{\text{PU,direct}}$ of the direct PU link, given by

$$\begin{aligned}\mathsf{C}_{\text{PU,direct}} &= \frac{1}{M}\sum_{m\in\mathcal{I}_{\text{PU,uc}}}\mathsf{E}\left[\log_2\left(1+\frac{\mathsf{P}_{\text{PU}}\,|H_{13}(m)|^2}{\sigma_{v_3}^2}\right)\right]\\ &= \frac{Q\,\log_2(e)}{M}\,\Psi(\mathsf{ASNR}_{13,\text{direct}})\end{aligned} \tag{27}$$

where $\mathsf{ASNR}_{13,\text{direct}} \triangleq (\sigma_{13}^2\,\mathsf{P}_{\text{PU}})/\sigma_{v_3}^2$ is the average SNR at the PRx when $\boldsymbol{\mathcal{A}} = \boldsymbol{\mathcal{G}} = \mathbf{O}_{M\times N}$, $\Psi(A) \triangleq \int_0^{+\infty} e^{-u}\,\ln(1+A\,u)\,\mathrm{d}u$,[20] with $A>0$, and we have used the fact that $|H_{13}(m)|^2$ has an exponential distribution with mean σ_{13}^2.

The degree of difficulty in evaluating the expectation in (26) depends on the choice of the precoding matrix $\boldsymbol{\Delta}$, which might be optimized to enhance the performance of the SU system and, hence, may be a function of the relevant channel coefficients (see Section IV). To obtain easily interpretable analytical results, we assume that $\{\|\boldsymbol{\alpha}_m\|^2\}_{m\in\mathcal{I}_{\text{PU,uc}}}$ and $\{\|\boldsymbol{\gamma}_m\|^2\}_{m\in\mathcal{I}_{\text{PU,vc}}}$ are independent on the realization of the channels, which happens, e.g., when a uniform power allocation strategy is employed by the STx over its used subcarriers. In this case, it is useful to observe from (16) that, conditioned on $H_{23}(m)\,F^{(n)}(m)$, one obtains that $H_{\text{PU}}(m)$ is a ZMCSCG random variable with variance $\sigma_{13}^2+\sigma_{12}^2\,|H_{23}(m)|^2\,|F^{(n)}(m)|^2$, $\forall m\in\{0,1,\ldots,M-1\}$, whose squared magnitude is exponentially distributed with mean $\sigma_{13}^2+\sigma_{12}^2\,|H_{23}(m)|^2\,|F^{(n)}(m)|^2$. By applying the conditional expectation rule [28], one has

$$\mathsf{C}_{\text{PU}} \geq \mathsf{C}_{\text{PU,lower}} = \frac{\log_2(e)}{M}\sum_{m\in\mathcal{I}_{\text{PU,uc}}}\mathsf{E}[\Psi(\Gamma_{3,m})] \tag{28}$$

with

$$\Gamma_{3,m} \triangleq \mathsf{ASNR}_{13,\text{direct}}\,\frac{1+|H_{23}(m)|^2\,|\boldsymbol{\alpha}_m^{\text{H}}\,\mathbf{x}_{\text{SU,I}}|^2\,\frac{\sigma_{12}^2}{\sigma_{13}^2}}{1+\|\boldsymbol{\alpha}_m\|^2\,\sigma_{23}^2\,\frac{\sigma_{v_2}^2}{\sigma_{v_3}^2}} \tag{29}$$

[20]It is seen [27] that

$$\Psi(A) = -e^{\frac{1}{A}}\,\mathrm{Ei}\left(-\frac{1}{A}\right) \approx \begin{cases} A\,, & \text{for } 0<A\ll 1;\\ \ln(1+A)-\gamma\,, & \text{for } A\gg 1.\end{cases}$$

where, for $x<0$,

$$\mathrm{Ei}(x) \triangleq \int_{-\infty}^{x}\frac{e^u}{u}\,\mathrm{d}u = \gamma+\ln(-x)+\sum_{k=1}^{+\infty}\frac{x^k}{k!\,k}$$

denotes the exponential integral function and $\gamma \triangleq \lim_{n\to\infty}\left(n^{-1}\sum_{k=1}^{n}k^{-1}-\ln n\right)\approx 0.57721$ is the Euler-Mascheroni constant.

where we have remembered that $F^{(n)}(m) = \boldsymbol{\alpha}_m^{\mathrm{H}}\,\mathbf{x}_{\mathrm{SU,I}}$. The lower bound (28) boils down to that reported in [12], [13] when $M_{\mathrm{vc}} = 0$, $L_{\mathrm{SU}} = 0$ or, equivalently, $N = 1$, $\boldsymbol{\alpha}_m \equiv \alpha_m = 1$, and $\boldsymbol{\gamma}_m \equiv \gamma_m = 0$, for each $m \in \{0, 1, \ldots, M-1\}$.

The numerator in (29) is the gain (with respect to the direct PU link) due to AF relaying, whereas its denominator is the performance loss caused by noise propagation from the STx to the PRx. As intuitively expected, if the SU does not transmit over all the Q subcarriers used by the PU (*conventional CR scenario*), i.e., $\boldsymbol{\alpha}_m = \mathbf{0}_N$ for each $m \in \mathcal{I}_{\mathrm{PU,uc}}$, one has $\Gamma_{3,m} = \mathsf{ASNR}_{13,\mathrm{direct}}$ and, hence, $\mathsf{C}_{\mathrm{PU}} = \mathsf{C}_{\mathrm{PU,direct}}$. In contrast, in our framework, the mth subcarrier is simultaneously used by both the PU and the SU, with $m \in \mathcal{I}_{\mathrm{PU,uc}}$. By resorting to the law of total expectation [28], it results that

$$\mathsf{E}[\Psi(\Gamma_{3,m})] = \mathsf{E}[\Psi(\Gamma_{3,m}) \,|\, \Gamma_{3,m} \geq \mathsf{ASNR}_{13,\mathrm{direct}}]\,[1 - \mathsf{Prob}(\Gamma_{3,m} < \mathsf{ASNR}_{13,\mathrm{direct}})] + \mathsf{E}[\Psi(\Gamma_{3,m}) \,|\, \Gamma_{3,m} < \mathsf{ASNR}_{13,\mathrm{direct}}]\,\mathsf{Prob}(\Gamma_{3,m} < \mathsf{ASNR}_{13,\mathrm{direct}})\,. \quad (30)$$

It is noteworthy that, if $\mathsf{Prob}(\Gamma_{3,m} < \mathsf{ASNR}_{13,\mathrm{direct}}) \to 0$, then

$$\mathsf{E}[\Psi(\Gamma_{3,m})] = \mathsf{E}[\Psi(\Gamma_{3,m}) \,|\, \Gamma_{3,m} \geq \mathsf{ASNR}_{13,\mathrm{direct}}] \geq \Psi(\mathsf{ASNR}_{13,\mathrm{direct}})\,, \quad \forall m \in \mathcal{I}_{\mathrm{PU,uc}} \quad (31)$$

where the inequality comes from the fact that $\Psi(A)$ is a monotonically increasing function of $A \geq 0$. Bearing in mind (27) and (28), inequality (31) implies that $\mathsf{C}_{\mathrm{PU}} \geq \mathsf{C}_{\mathrm{PU,direct}}$. Remarkably, in the presence of the concurrent SU transmission, the capacity of the PU cannot degrade if $\mathsf{Prob}(\Gamma_{3,m} < \mathsf{ASNR}_{13,\mathrm{direct}})$ is negligibly small. Therefore, we say that the PU system is in *outage* when $\Gamma_{3,m} < \mathsf{ASNR}_{13,\mathrm{direct}}$ and we will refer to $\mathsf{Prob}_{\mathrm{PU,out},m} \triangleq \mathsf{Prob}(\Gamma_{3,m} < \mathsf{ASNR}_{13,\mathrm{direct}})$ as the *outage probability* of the PU system. Evaluation of $\mathsf{Prob}_{\mathrm{PU,out},m}$ requires the calculation of the cumulative distribution function $p_m(z) \triangleq P(|H_{23}(m)|^2\,|\boldsymbol{\alpha}_m^{\mathrm{H}}\,\mathbf{x}_{\mathrm{SU,I}}|^2 \leq z)$ of the random variable $|H_{23}(m)|^2\,|\boldsymbol{\alpha}_m^{\mathrm{H}}\,\mathbf{x}_{\mathrm{SU,I}}|^2$, with $z \geq 0$. To this aim, we remember that $H_{23}(m)$ is a ZMCSCG random variable with variance σ_{23}^2 and, hereinafter, we additionally assume that $\mathbf{x}_{\mathrm{SU,I}}$ is a ZMCSCG random vector with correlation matrix $\mathsf{E}[\mathbf{x}_{\mathrm{SU,I}}\,\mathbf{x}_{\mathrm{SU,I}}^{\mathrm{H}}] = \mathbf{I}_Q$. Consequently, it results that $|H_{23}(m)|^2$ and $|\boldsymbol{\alpha}_m^{\mathrm{H}}\,\mathbf{x}_{\mathrm{SU,I}}|^2$ are independent exponential random variables with mean σ_{23}^2 and $\|\boldsymbol{\alpha}_m\|^2$, respectively, which leads to $p_m(z) \equiv 0$ for $z < 0$, whereas (see, e.g., [28])

$$p_m(z) = 1 - \frac{1}{\sigma_{23}^2}\int_0^{+\infty} e^{-\left(\frac{x}{\sigma_{23}^2} + \frac{z}{x\,\|\boldsymbol{\alpha}_m\|^2}\right)}\,\mathrm{d}x = 1 - \frac{2\sqrt{z}}{\sigma_{23}\,\|\boldsymbol{\alpha}_m\|}\,K_1\left(\frac{2\sqrt{z}}{\sigma_{23}\,\|\boldsymbol{\alpha}_m\|}\right) \quad (z \geq 0) \quad (32)$$

where $K_\alpha(x)$ is the modified Bessel function of the third kind and order α, with $x > 0$.[21] Accounting for (29), it follows that

$$\mathsf{Prob}_{\text{PU,out},m} = p_m\left(\|\boldsymbol{\alpha}_m\|^2\,\frac{\sigma_{23}^2\,\sigma_{13}^2}{\sigma_{12}^2}\,\frac{\sigma_{v_2}^2}{\sigma_{v_3}^2}\right) = 1 - 2\,\frac{\sigma_{13}}{\sigma_{12}}\,\frac{\sigma_{v_2}}{\sigma_{v_3}}\,K_1\left(2\,\frac{\sigma_{13}}{\sigma_{12}}\,\frac{\sigma_{v_2}}{\sigma_{v_3}}\right). \tag{33}$$

It is noteworthy that the outage probability of the PU system does not depend on the precoding matrix of the STx and $\mathsf{Prob}_{\text{PU,out},m} \equiv \mathsf{Prob}_{\text{PU,out}}$. Henceforth, the following mathematical condition

$$2\,\frac{\sigma_{13}}{\sigma_{12}}\,\frac{\sigma_{v_2}}{\sigma_{v_3}}\,K_1\left(2\,\frac{\sigma_{13}}{\sigma_{12}}\,\frac{\sigma_{v_2}}{\sigma_{v_3}}\right) \to 1 \tag{34}$$

ensures that the outage probability of the PU system tends to zero and, thus, $\mathsf{C}_{\text{PU}} \geq \mathsf{C}_{\text{PU,direct}}$.

In order to find the solution of eq. (34) with respect to $x \equiv 2\,(\sigma_{13}/\sigma_{12})\,(\sigma_{v_2}/\sigma_{v_3})$, it is useful to consider the limiting form of the Bessel function $K_1(x)$ for small argument: when $x \to 0$, it results [29, Eq. 9.7.2] that $K_1(x) \sim 1/x$; therefore, equation $x\,K_1(x) \to 1$ is satisfied for x close to zero. This implies that eq. (34) is fulfilled when

$$\frac{\sigma_{13}}{\sigma_{12}}\,\frac{\sigma_{v_2}}{\sigma_{v_3}} \to 0 \tag{35}$$

that is, in practical terms, when σ_{13}/σ_{12} is much smaller than $\sigma_{v_3}/\sigma_{v_2}$. In this case, it is interesting to observe from (29) that $\mathsf{E}(\Gamma_{3,m})$ turns out to be much greater than $\mathsf{ASNR}_{13,\text{direct}}$. In other words, to achieve the performance gain $\mathsf{C}_{\text{PU}} \geq \mathsf{C}_{\text{PU,direct}}$, the favourable effect of AF relaying has to be predominant *on average* with respect to the adverse phenomenon of noise propagation.

Let us specialize condition (35) to a case of practical interest. To this end, we assume that: (i) $\sigma_{i\ell}^2 = d_{i\ell}^{-\eta}$, where $d_{i\ell}$ is the distance between nodes i and ℓ, and η denotes the path-loss exponent; (ii) nodes 2 and 3 (approximatively) have the same noise figure, i.e., $\sigma_{v_2}^2 \approx \sigma_{v_3}^2$. Under these assumptions, condition (35) ends up to $d_{12}/d_{13} \to 0$: the outage probability of the PU system is vanishingly small when the distance d_{13} between the PTx and the PRx is significantly greater than the distance between the PTx and the STx (see Fig. 1).

[21] As by definition (see, e.g., [29])

$$K_\alpha(x) \triangleq \frac{\sqrt{\pi}\,x^\alpha}{2^\alpha\,\Gamma(\alpha+1/2)}\int_0^{+\infty} e^{-x\,t}\,(t^2-1)^{\alpha-1/2}\,\mathrm{d}t$$

where $\Gamma(x) \triangleq \int_0^{+\infty} t^{x-1}\,e^{-t}\,\mathrm{d}t$ is the Gamma function. It results that $\Gamma(1/2) = \sqrt{\pi}$ and $\Gamma(3/2) = \sqrt{\pi}/2$. Moreover, for any $p > 0$ and $q > 0$, it results that (see [30, Eq. 2.3.16.1])

$$\int_0^{+\infty} x^{\alpha-1}\,e^{-\left(p\,x+\frac{q}{x}\right)}\,\mathrm{d}x = 2\left(\frac{q}{p}\right)^{\alpha/2} K_\alpha(2\sqrt{p\,q})\,.$$

A final remark is now in order regarding the dependence of $\mathsf{C}_{\text{PU,lower}}$ on the power budget P_{SU} of the SU. Accounting for (23), it follows that, $\forall m \in \mathcal{M}$,

$$\|\boldsymbol{\alpha}_m\|^2 = \frac{\mathsf{P}_{\text{SU}} - \sum_{\ell \in \mathcal{I}_{\text{PU,vc}}} \|\boldsymbol{\gamma}_\ell\|^2}{\sigma_{12}^2\, \mathsf{P}_{\text{PU}} + \sigma_{v_2}^2} - \sum_{\substack{\ell \,\in\, \mathcal{I}_{\text{PU,uc}} \\ \ell \neq m}} \|\boldsymbol{\alpha}_\ell\|^2 \tag{36}$$

The following Lemma unveils the relationship between $\mathsf{C}_{\text{PU,lower}}$ and P_{SU}:

Lemma 2: If (35) holds, then $\mathsf{C}_{\text{PU,lower}}$ in (28) is a monotonically increasing function of P_{SU}.

Proof: See Appendix A. ■

The statement of Lemma 2 is in contrast with conventional CR approaches [3], for which concurrent transmission of the SU is allowed only if its power is subject to a strict constraint. Such a result directly comes from the fact that the STx also acts as a relay for the PU system.

IV. Analysis of the ergodic capacity and precoding optimization of the SU

In this section, we investigate the information-theoretic performance of the SU and also discuss how the precoding matrices $\boldsymbol{\mathcal{C}}$ and $\boldsymbol{\mathcal{D}}$ can be optimized to enhance the achievable rate of the SU. Specifically, we assume that the SRx has perfect knowledge of the matrix $\boldsymbol{\mathcal{H}}_{\text{SU}}$, which can be estimated via training sent by the STx (see Subsection II-E).[22]

With reference to the signal model (20), the channel output is represented by the pair $(\mathbf{y}_{\text{SU}}, \boldsymbol{\mathcal{H}}_{\text{SU}})$ and, thus, the mutual information between channel input and output is given by $\mathsf{I}(\mathbf{x}_{\text{SU}}, \mathbf{y}_{\text{SU}} \,|\, \boldsymbol{\mathcal{H}}_{\text{SU}})$ (in bits/s/Hz). First, we calculate a lower bound on $\mathsf{I}(\mathbf{x}_{\text{SU}}, \mathbf{y}_{\text{SU}} \,|\, \boldsymbol{\mathcal{H}}_{\text{SU}})$, by considering the worst-case distribution for the equivalent noise term at the SRx under a variance constraint (see footnote 18), i.e., $\mathbf{v}_{\text{SU}}$ is modeled as a ZMCSCG random vector with (diagonal) correlation matrix $\mathbf{R}_{\mathbf{v}_{\text{SU}}} \triangleq \mathsf{E}[\mathbf{v}_{\text{SU}}\, \mathbf{v}_{\text{SU}}^{\text{H}}] = \mathsf{P}_{\text{PU}}\, \sigma_{14}^2\, \boldsymbol{\Theta}\, \boldsymbol{\Theta}^{\text{T}} + \sigma_{v_4}^2\, \mathbf{I}_M$. By assuming that $\mathbf{x}_{\text{SU}}$ is a ZMCSCG random vector, with correlation matrix $\mathsf{E}[\mathbf{x}_{\text{SU}}\, \mathbf{x}_{\text{SU}}^{\text{H}}] = \mathbf{I}_N$, it follows that $\mathsf{I}(\mathbf{x}_{\text{SU}}, \mathbf{y}_{\text{SU}} \,|\, \boldsymbol{\mathcal{H}}_{\text{SU}})$ under an average transmitter constraint is lower bounded as

$$\mathsf{I}(\mathbf{x}_{\text{SU}}, \mathbf{y}_{\text{SU}} \,|\, \boldsymbol{\mathcal{H}}_{\text{SU}}) \geq \mathsf{I}_{\min}(\mathbf{x}_{\text{SU}}, \mathbf{y}_{\text{SU}} \,|\, \boldsymbol{\mathcal{H}}_{\text{SU}}) \triangleq \frac{1}{M}\, \log_2 \left[\frac{\det(\mathbf{R}_{\mathbf{v}_{\text{SU}}} + \boldsymbol{\mathcal{H}}_{\text{SU}}\, \boldsymbol{\Omega}\, \boldsymbol{\mathcal{H}}_{\text{SU}}^{\text{H}})}{\det(\mathbf{R}_{\mathbf{v}_{\text{SU}}})} \right] \tag{37}$$

where $\mathsf{E}[\|\mathbf{x}_{\text{SU}}\|^2] = N + M_{\text{vc}}$ is the overall transmit power and $\mathbf{R}_{\mathbf{v}_{\text{SU}}}$ is nonsingular, i.e., $\det(\mathbf{R}_{\mathbf{v}_{\text{SU}}}) \neq 0$, for SNR values of practical interest, $\boldsymbol{\Omega} \triangleq \boldsymbol{\Delta}\, \boldsymbol{\Delta}^{\text{H}} \in \mathbb{C}^{2M \times 2M}$ is a positive-semidefinite Hermitian matrix.[23] It is noteworthy that the RHS of (37) is concave as a function

[22]This can be regarded as a *worst case*, since in practice the SRx might additionally have knowledge of the training symbols of the PU system, which may be used to estimate the channel impulse response over the $1 \rightarrow 4$ link, i.e., $\boldsymbol{\mathcal{H}}_{14}$.

[23]The set of positive-semidefinite matrices is a closed convex cone [20].

of $\boldsymbol{\Omega}$ [31, Thm. 1] and, therefore, it can be maximized with respect to $\boldsymbol{\Omega}$. To this aim, using the facts that $\det(\mathbf{B}_1\,\mathbf{B}_2) = \det(\mathbf{B}_1)\,\det(\mathbf{B}_2)$ and $\det(\mathbf{B}_1^{-1}) = 1/\det(\mathbf{B}_1)$, for $\mathbf{B}_1, \mathbf{B}_2 \in \mathbb{C}^{n\times n}$, it is readily seen that

$$\frac{\det(\mathbf{R}_{\mathbf{v}_{\text{SU}}} + \boldsymbol{\mathcal{H}}_{\text{SU}}\,\boldsymbol{\Omega}\,\boldsymbol{\mathcal{H}}_{\text{SU}}^{\text{H}})}{\det(\mathbf{R}_{\mathbf{v}_{\text{SU}}})} = \det(\mathbf{I}_M + \mathbf{R}_{\mathbf{v}_{\text{SU}}}^{-1}\,\boldsymbol{\mathcal{H}}_{\text{SU}}\,\boldsymbol{\Omega}\,\boldsymbol{\mathcal{H}}_{\text{SU}}^{\text{H}})\,. \tag{38}$$

By observing that $\mathbf{R}_{\mathbf{v}_{\text{SU}}}$ is diagonal by construction, Hadamard's inequality [20] implies that the RHS of (38) [and, hence, $\mathsf{I}_{\text{min}}(\mathbf{x}_{\text{SU}}, \mathbf{y}_{\text{SU}} \,|\, \boldsymbol{\mathcal{H}}_{\text{SU}})$] is maximized when

$$\boldsymbol{\mathcal{H}}_{\text{SU}}\,\boldsymbol{\Omega}\,\boldsymbol{\mathcal{H}}_{\text{SU}}^{\text{H}} = \mathbf{H}_{\text{SU}}\,\boldsymbol{\Pi}_{\text{IDFT}}\,\boldsymbol{\Upsilon}_{\text{vc}}\,\boldsymbol{\mathcal{C}}\,\boldsymbol{\mathcal{C}}^{\text{H}}\,\boldsymbol{\Upsilon}_{\text{vc}}^{\text{H}}\,\boldsymbol{\Pi}_{\text{IDFT}}^{\text{H}}\,\mathbf{H}_{\text{SU}}^{\text{H}} + \boldsymbol{\mathcal{H}}_{24}\,\boldsymbol{\Xi}\,\boldsymbol{\mathcal{D}}\,\boldsymbol{\mathcal{D}}^{\text{H}}\,\boldsymbol{\Xi}^{\text{T}}\,\boldsymbol{\mathcal{H}}_{24}^{\text{H}} \tag{39}$$

is a diagonal matrix. Since $\mathbf{H}_{\text{SU}}$ [see eq. (21)] and $\boldsymbol{\mathcal{H}}_{24}$ are diagonal matrices, maximization of $\mathsf{I}_{\text{min}}(\mathbf{x}_{\text{SU}}, \mathbf{y}_{\text{SU}} \,|\, \boldsymbol{\mathcal{H}}_{\text{SU}})$ can be obtained by imposing that the matrices $\boldsymbol{\Pi}_{\text{IDFT}}\,\boldsymbol{\Upsilon}_{\text{vc}}\,\boldsymbol{\mathcal{C}}\,\boldsymbol{\mathcal{C}}^{\text{H}}\,\boldsymbol{\Upsilon}_{\text{vc}}^{\text{H}}\,\boldsymbol{\Pi}_{\text{IDFT}}^{\text{H}}$ and $\boldsymbol{\Xi}\,\boldsymbol{\mathcal{D}}\,\boldsymbol{\mathcal{D}}^{\text{H}}\,\boldsymbol{\Xi}^{\text{T}}$ are diagonal, too. Therefore, we impose that $\boldsymbol{\Pi}_{\text{IDFT}}\,\boldsymbol{\Upsilon}_{\text{vc}}\,\boldsymbol{\mathcal{C}}\,\boldsymbol{\mathcal{C}}^{\text{H}}\,\boldsymbol{\Upsilon}_{\text{vc}}^{\text{H}}\,\boldsymbol{\Pi}_{\text{IDFT}}^{\text{H}} = \boldsymbol{\Sigma}_{\boldsymbol{\mathcal{A}}}$ and $\boldsymbol{\Xi}\,\boldsymbol{\mathcal{D}}\,\boldsymbol{\mathcal{D}}^{\text{H}}\,\boldsymbol{\Xi}^{\text{T}} = \boldsymbol{\Sigma}_{\boldsymbol{\mathcal{G}}}$, where $\boldsymbol{\Sigma}_{\boldsymbol{\mathcal{A}}}$ and $\boldsymbol{\Sigma}_{\boldsymbol{\mathcal{G}}}$ have been previously defined in (24), whose particular solutions can be expressed as

$$\boldsymbol{\mathcal{C}}\,\boldsymbol{\mathcal{C}}^{\text{H}} = \boldsymbol{\Upsilon}_{\text{vc}}^{\text{H}}\,\boldsymbol{\Pi}_{\text{IDFT}}^{\text{H}}\,\boldsymbol{\Sigma}_{\boldsymbol{\mathcal{A}}}\,\boldsymbol{\Pi}_{\text{IDFT}}\,\boldsymbol{\Upsilon}_{\text{vc}} \tag{40}$$

$$\boldsymbol{\mathcal{D}}\,\boldsymbol{\mathcal{D}}^{\text{H}} = \boldsymbol{\Xi}^{\text{T}}\,\boldsymbol{\Sigma}_{\boldsymbol{\mathcal{G}}}\,\boldsymbol{\Xi}\,. \tag{41}$$

In this case, by virtue of (37), (39), (40), and (41), and remembering that we have imposed $\boldsymbol{\alpha}_m = \mathbf{0}_N$, $\forall m \in \mathcal{I}_{\text{PU,vc}}$, and $\boldsymbol{\gamma}_m = \mathbf{0}_{M_{\text{vc}}}$, $\forall m \in \mathcal{I}_{\text{PU,uc}}$, one has

$$\mathsf{I}_{\text{min}}(\mathbf{x}_{\text{SU}}, \mathbf{y}_{\text{SU}} \,|\, \boldsymbol{\mathcal{H}}_{\text{SU}}) = \frac{1}{M}\left[\sum_{m\in\mathcal{I}_{\text{PU,uc}}} \log_2\left(1 + \frac{|H_{\text{SU}}(m)|^2\,\|\boldsymbol{\alpha}_m\|^2}{\sigma_{14}^2\,\mathsf{P}_{\text{PU}} + \sigma_{v_4}^2}\right) + \sum_{m\in\mathcal{I}_{\text{PU,vc}}} \log_2\left(1 + \frac{|H_{24}(m)|^2\,\|\boldsymbol{\gamma}_m\|^2}{\sigma_{v_4}^2}\right)\right]\,. \tag{42}$$

By averaging $\mathsf{I}(\mathbf{x}_{\text{SU}}, \mathbf{y}_{\text{SU}} \,|\, \boldsymbol{\mathcal{H}}_{\text{SU}})$ with respect to the relevant channel parameters, and relying on (37) and (42), the ergodic capacity C_{SU} of the SU can be lower bounded as follows

$$\mathsf{C}_{\text{SU}} \triangleq \mathsf{E}[\mathsf{I}(\mathbf{x}_{\text{SU}}, \mathbf{y}_{\text{SU}} \,|\, \boldsymbol{\mathcal{H}}_{\text{SU}})] \geq \mathsf{C}_{\text{SU,lower}} \triangleq \mathsf{E}\left[\mathsf{I}_{\text{min}}(\mathbf{x}_{\text{SU}}, \mathbf{y}_{\text{SU}} \,|\, \boldsymbol{\mathcal{H}}_{\text{SU}})\right]\,. \tag{43}$$

It is worth noticing that the capacity of the SU is essentially limited by the variance $\sigma_{14}^2\,\mathsf{P}_{\text{PU}} + \sigma_{v_4}^2$ of the equivalent noise term $\mathbf{v}_{\text{SU}}$ at the SRx (see Subsection II-E). Evaluation of the expectation in (43) depends on the choice of the scalar variables $a_m \triangleq \|\boldsymbol{\alpha}_m\|^2$, for $m \in \mathcal{I}_{\text{PU,uc}}$, and $g_m \triangleq \|\boldsymbol{\gamma}_m\|^2$, for $m \in \mathcal{I}_{\text{PU,vc}}$, which in its turn may depend on the CSI at the transmitter (CSIT) of the SU system. In the following two subsections, we separately consider two relevant scenarios.

A. CSIT scenario

In this scenario, the STx has perfect knowledge of the channel matrix $\boldsymbol{\mathcal{H}}_{\text{SU}}$, which allows one to further maximize the mutual information between channel input and output. Channel estimation at the transmitter requires either a feedback channel or the application of the channel reciprocity property when the same carrier frequency is used for transmission and reception. Henceforth, accounting for (42), we propose to solve the following optimization problem

$$\arg \max_{\substack{\{a_m\}_{m\in\mathcal{I}_{\text{PU,uc}}} \\ \{g_m\}_{m\in\mathcal{I}_{\text{PU,vc}}}}} \left[\sum_{m\in\mathcal{I}_{\text{PU,uc}}} \log_2 \left(1 + \frac{|H_{\text{SU}}(m)|^2 \, a_m}{\sigma_{14}^2 \, \mathsf{P}_{\text{PU}} + \sigma_{v_4}^2} \right) + \sum_{m\in\mathcal{I}_{\text{PU,vc}}} \log_2 \left(1 + \frac{|H_{24}(m)|^2 \, g_m}{\sigma_{v_4}^2} \right) \right] \tag{44}$$

subject to the power constraint [see (23)]

$$(\sigma_{12}^2 \, \mathsf{P}_{\text{PU}} + \sigma_{v_2}^2) \sum_{m\in\mathcal{I}_{\text{PU,uc}}} a_m + \sum_{m\in\mathcal{I}_{\text{PU,vc}}} g_m = \mathsf{P}_{\text{SU}} \, . \tag{45}$$

The solution of such a problem is given by the following Lemma:

Lemma 3: Problem (44)–(45) admits the following *waterfilling* solution

$$a_{m,\text{opt}} = \left[\mu - \frac{\sigma_{14}^2 \, \mathsf{P}_{\text{PU}} + \sigma_{v_4}^2}{|H_{\text{SU}}(m)|^2} \right]^+ , \quad \forall m \in \mathcal{I}_{\text{PU,uc}} \tag{46}$$

$$g_{m,\text{opt}} = \left[\mu - \frac{\sigma_{v_4}^2}{|H_{24}(m)|^2} \right]^+ , \quad \forall m \in \mathcal{I}_{\text{PU,vc}} \tag{47}$$

where the constant μ is chosen so as to fulfil the constraint

$$(\sigma_{12}^2 \, \mathsf{P}_{\text{PU}} + \sigma_{v_2}^2) \sum_{m\in\mathcal{I}_{\text{PU,uc}}} \left[\mu - \frac{\sigma_{14}^2 \, \mathsf{P}_{\text{PU}} + \sigma_{v_4}^2}{|H_{\text{SU}}(m)|^2} \right]^+ + \sum_{m\in\mathcal{I}_{\text{PU,vc}}} \left[\mu - \frac{\sigma_{v_4}^2}{|H_{24}(m)|^2} \right]^+ = \mathsf{P}_{\text{SU}} \, . \tag{48}$$

Proof: The proof is obtained by using standard optimization concepts (see, e.g., [32]). ■

In such a CSIT scenario, the worst-case ergodic channel capacity of the SU can be obtained by replacing in (42)–(43) $\|\boldsymbol{\alpha}_m\|^2$ and $\|\boldsymbol{\gamma}_m\|^2$ with $a_{m,\text{opt}}$ and $g_{m,\text{opt}}$, respectively, thus obtaining

$$\mathsf{C}_{\text{SU,lower,CSIT}} = \frac{1}{M} \left\{ \sum_{m\in\mathcal{I}_{\text{PU,uc}}} \mathsf{E} \left[\left(\log_2 \left(\frac{\mu \, |H_{\text{SU}}(m)|^2}{\sigma_{14}^2 \, \mathsf{P}_{\text{PU}} + \sigma_{v_4}^2} \right) \right)^+ \right] \right.$$
$$\left. + \sum_{m\in\mathcal{I}_{\text{PU,vc}}} \mathsf{E} \left[\left(\log_2 \left(\frac{\mu \, |H_{24}(m)|^2}{\sigma_{v_4}^2} \right) \right)^+ \right] \right\} . \tag{49}$$

Let us assume for simplicity that nodes 2 and 4 (approximatively) have the same noise figure, i.e., $\sigma^2 = \sigma_{v_2}^2 \approx \sigma_{v_4}^2$, it is readily verified that, even in the presence of CSIT, the first summand of the ergodic channel capacity $\mathsf{C}_{\text{SU,lower,CSIT}}$ tends to a bounded quantity as $\sigma^2 \to 0$. In other words, maximization of the mutual information between channel input and output does not allow to cope with the interference generated by the PU on the SU system over the $1 \to 4$ link.

B. No CSIT (NOCSIT) scenario

In this scenario, CSIT is not available at the STx. In such a case, a viable choice consists of uniformly allocating the power over the subcarriers used by the SU, i.e., $\|\boldsymbol{\alpha}_m\|^2 \equiv a > 0$ for each $m \in \mathcal{I}_{\text{PU,uc}}$ and $\|\boldsymbol{\gamma}_m\|^2 \equiv g > 0$ for each $m \in \mathcal{I}_{\text{PU,vc}}$. In this case, eq. (36) ends up to

$$a = \frac{\mathsf{P}_{\text{SU}} - M_{\text{vc}}\, g}{Q\,(\sigma_{12}^2\, \mathsf{P}_{\text{PU}} + \sigma_{v_2}^2)}\,. \tag{50}$$

Accounting for (21) and (43), the expectation of the first summand of $\mathsf{I}_{\text{min}}(\mathbf{x}_{\text{SU}}, \mathbf{y}_{\text{SU}} \,|\, \boldsymbol{\mathcal{H}}_{\text{SU}})$ in (42) can be evaluated by exploiting the statistical independence between $H_{12}(m)$ and $v_2(m)$: indeed, conditioned on $H_{24}(m)$ and $x_{\text{PU}}(m)$, $H_{\text{SU}}(m)$ is a ZMCSCG random variable having variance $|H_{24}(m)|^2\,(\sigma_{12}^2\,|x_{\text{PU}}(m)|^2 + \sigma_{v_2}^2)$, for each $m \in \mathcal{I}_{\text{PU,uc}}$, whose squared magnitude is exponentially distributed with mean $|H_{24}(m)|^2\,(\sigma_{12}^2\,|x_{\text{PU}}(m)|^2 + \sigma_{v_2}^2)$. Therefore, it results from (42)–(43) that

$$\mathsf{C}_{\text{SU,lower,NOCSIT}} = \frac{\log_2(e)}{M}\left\{\sum_{m\in\mathcal{I}_{\text{PU,uc}}} \mathsf{E}[\Psi(\Gamma_{4,m})] + M_{\text{vc}}\,\Psi(\mathsf{ASNR}_{24,\text{direct}})\right\} \tag{51}$$

with

$$\Gamma_{4,m} \triangleq \frac{|H_{24}(m)|^2\,(\sigma_{12}^2\,|x_{\text{PU}}(m)|^2 + \sigma_{v_2}^2)\,(\mathsf{P}_{\text{SU}} - M_{\text{vc}}\, g)}{Q\,(\sigma_{14}^2\,\mathsf{P}_{\text{PU}} + \sigma_{v_4}^2)\,(\sigma_{12}^2\,\mathsf{P}_{\text{PU}} + \sigma_{v_2}^2)} \tag{52}$$

and $\mathsf{ASNR}_{24,\text{direct}} \triangleq (\sigma_{24}^2\, g)/\sigma_{v_4}^2$ representing the average SNR of the direct link between STx and SRx, where we have accounted for (36) and, regarding the second summand of $\mathsf{I}_{\text{min}}(\mathbf{x}_{\text{SU}}, \mathbf{y}_{\text{SU}} \,|\, \widetilde{\mathbf{H}}_{\text{SU}})$ in (42), we have used the fact that $|H_{24}(m)|^2$ has an exponential distribution with mean σ_{24}^2.

A particularization of (51) can be obtained by assuming that the PU symbols are drawn from a constant-modulus constellation, i.e., $|x_{\text{PU}}(m)|^2 = \mathsf{P}_{\text{PU}}$. In this case, when $\Gamma_{4,m}$ assumes negligible values on average, i.e., $\mathsf{P}_{\text{SU}} - M_{\text{vc}}\, g \ll Q\,(\sigma_{14}^2\,\mathsf{P}_{\text{PU}} + \sigma_{v_4}^2)/\sigma_{24}^2$, one obtains that (see footnote 20)

$$\begin{aligned}\mathsf{C}_{\text{SU,lower,NOCSIT}} &\approx \frac{\log_2(e)}{M}\left[\sum_{m\in\mathcal{I}_{\text{PU,uc}}} \mathsf{E}(\Gamma_{4,m}) + M_{\text{vc}}\,\Psi(\mathsf{ASNR}_{24,\text{direct}})\right] \\ &= \frac{\log_2(e)}{M}\left[\mathsf{ASNR}_{24,\text{direct}}\,\frac{\frac{\mathsf{P}_{\text{SU}}}{g} - M_{\text{vc}}}{1 + \mathsf{ASNR}_{14,\text{direct}}} + M_{\text{vc}}\,\Psi(\mathsf{ASNR}_{24,\text{direct}})\right]\end{aligned} \tag{53}$$

with $\mathsf{ASNR}_{14,\text{direct}} \triangleq (\sigma_{14}^2\,\mathsf{P}_{\text{PU}})/\sigma_{v_4}^2$ representing the average SNR of the direct link between PTx and SRx. On the contrary, when $\Gamma_{4,m}$ assumes large values on average, i.e., $\mathsf{P}_{\text{SU}} - M_{\text{vc}}\, g \gg$

$Q\,(\sigma_{14}^2\,\mathsf{P}_{\text{PU}}+\sigma_{v_4}^2)/\sigma_{24}^2$, one gets that (see footnote 20 again)

$$\begin{aligned}\mathsf{C}_{\text{SU,lower,NOCSIT}} &\approx \frac{\log_2(e)}{M}\left\{\sum_{m\in\mathcal{I}_{\text{PU,uc}}}\mathsf{E}[(\ln(1+\Gamma_{4,m})-\gamma]+M_{\text{vc}}\,\Psi(\mathsf{ASNR}_{24,\text{direct}})\right\}\\ &= \frac{\log_2(e)}{M}\left[\Psi\left(\frac{\mathsf{ASNR}_{24,\text{direct}}}{Q}\,\frac{\frac{\mathsf{P}_{\text{SU}}}{g}-M_{\text{vc}}}{1+\mathsf{ASNR}_{14,\text{direct}}}\right)-\gamma\,Q+M_{\text{vc}}\,\Psi(\mathsf{ASNR}_{24,\text{direct}})\right]. \end{aligned} \tag{54}$$

As it is apparent from (53) and (54), due to the equivalent noise term $\mathbf{v}_{\text{SU}}$ at the SRx (see Subsection II-E), the worst-case capacity of the SU is inversely related to the average SNR over the direct link between the PTx and the SRx, which might be a limiting factor for the SU ergodic capacity. Such a potential trouble can be circumvented by allowing the SRx to estimate the PU symbol block $\mathbf{x}_{\text{PU}}$ and, consequently, subtract its contribution from the received data. This requires knowledge at the SRx of the training protocol of the PU.

V. Numerical performance analysis

To corroborate our information-theoretic analysis, we report some results of numerical simulations. With reference to Fig. 1, we normalize the distance between the PTx and the PRx, as well as the transmitting power of the PU, by setting $d_{13}=1$ and $\mathsf{P}_{\text{PU}}=1$, respectively. Specifically, the nodes 1 (PTx), 3 (PRx), and 4 (SRx) have coordinates equal to $(-0.5,0)$, $(0.5,0)$, and $(0,2)$, respectively. In all the plots where the distance d_{12} varies, the node 2 (STx) moves along the line joining the nodes 1 and 2, with $\vartheta=\pi/3$ (see Fig. 1). The memory of the discrete-time channels among the nodes is set equal to $L_{12}=1$, $L_{13}=L_{14}=3$, and $L_{24}=L_{23}=2$, whereas the corresponding time offsets are fixed to $\theta_{12}=1$, $\theta_{13}=\theta_{14}=3$, and $\theta_{24}=\theta_{23}=2$, respectively. The path-loss exponent is chosen equal to $\eta=3$. According to (14) and (19), we choose $L_{\text{SU}}=10$, which leads to $N=L_{\text{SU}}-M_{\text{vc}}+1=7$. The symbol blocks $\mathbf{x}_{\text{PU}}$ and $\mathbf{x}_{\text{SU}}$ are ZMCSCG random vectors, with correlation matrices $\mathsf{P}_{\text{PU}}\,\mathbf{I}_Q$ and $\mathsf{P}_{\text{SU}}\,\mathbf{I}_{N+M_{\text{vc}}}$, respectively. Moreover, we set $\sigma_{v_2}^2=\sigma_{v_3}^2=\sigma_{v_4}^2=\sigma^2$. The ensemble averages (with respect to the fading channels and information-bearing symbols) in (28), (49), and (51) are evaluated through 10^6 Monte Carlo trials.

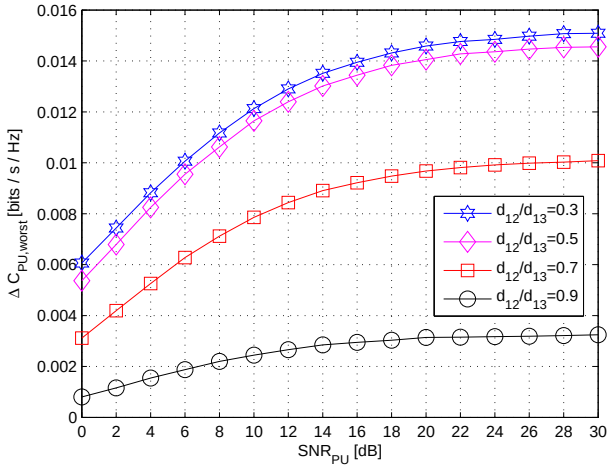

Figure 3. $\Delta \mathsf{C}_{\mathrm{PU,worst}}$ versus $\mathsf{SNR}_{\mathrm{PU}}$ for different values of d_{12}/d_{13} ($\mathsf{P}_{\mathrm{SU}}/\mathsf{P}_{\mathrm{PU}} = 1$).

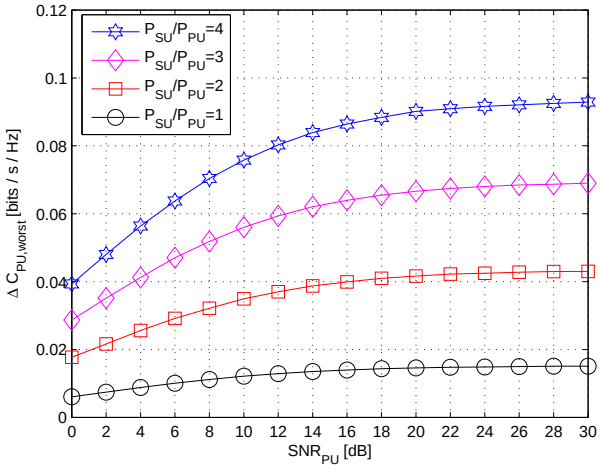

Figure 4. $\Delta \mathsf{C}_{\mathrm{PU,worst}}$ versus $\mathsf{SNR}_{\mathrm{PU}}$ for different values of $\mathsf{P}_{\mathrm{SU}}/\mathsf{P}_{\mathrm{PU}}$ ($d_{12}/d_{13} = 0.3$).

A. Performance of the primary system

Herein, we study the worst-case performance of the primary system, by assuming a uniform power allocation for the SU transmission,[24] i.e., $\|\boldsymbol{\alpha}_m\|^2 \equiv a > 0$, for each $m \in \mathcal{I}_{\mathrm{PU,uc}}$, and $\|\boldsymbol{\gamma}_m\|^2 \equiv g > 0$, for each $m \in \mathcal{I}_{\mathrm{PU,vc}}$, fulfil (50), with $\mathsf{P}_{\mathrm{SU}}/\mathsf{P}_{\mathrm{PU}} = 1$ and $g = \mathsf{P}_{\mathrm{SU}}/(2\,M_{\mathrm{vc}})$.

Figs. 3 and 4 depict the (minimum) capacity gain $\Delta \mathsf{C}_{\mathrm{PU,worst}} \triangleq \mathsf{C}_{\mathrm{PU,lower}} - \mathsf{C}_{\mathrm{PU,direct}}$ of the PU as a function of $\mathsf{SNR}_{\mathrm{PU}} \triangleq \mathsf{P}_{\mathrm{PU}}/\sigma^2$. Specifically, different values of the ratio d_{12}/d_{13} are considered in Fig. 3, with $\mathsf{P}_{\mathrm{SU}}/\mathsf{P}_{\mathrm{PU}} = 1$, whereas the curves in Fig. 4 are reported for different values of the power ratio $\mathsf{P}_{\mathrm{SU}}/\mathsf{P}_{\mathrm{PU}}$, with $d_{12}/d_{13} = 0.3$. Results show that the PU can unknowingly attain a capacity gain from the concurrent transmission of the SU, which significantly increases either when the SU is getting closer and closer to the PU or when the SU system has a power budget to spend greater than that of the PU one. For instance, let us consider the case of a primary Wi-Fi system with $1/T_c = 20$ MHz: when $\mathsf{P}_{\mathrm{PU}} = \mathsf{P}_{\mathrm{SU}}$ and $d_{12}/d_{13} = 0.3$, it results from Fig. 3 that the capacity gain is at least equal to 300 kbps at $\mathsf{SNR}_{\mathrm{PU}} > 20$ dB, whereas, when the STx spends twice as much power as the PTx, such a gain amounts at least to 1.8 Mbps (see Fig. 4).

B. Performance of the secondary system

In this subsection, we focus on the (minimum) achievable rate $\mathsf{C}_{\mathrm{SU,lower}}$ of the SU [see (43)]. In particular, we consider the case when CSI is available at the STx by depicting $\mathsf{C}_{\mathrm{SU,lower,CSIT}}$ in

[24]Results non reported here show that the performance of the PU is not significantly influenced on the way the SU encodes its information-bearing symbols.

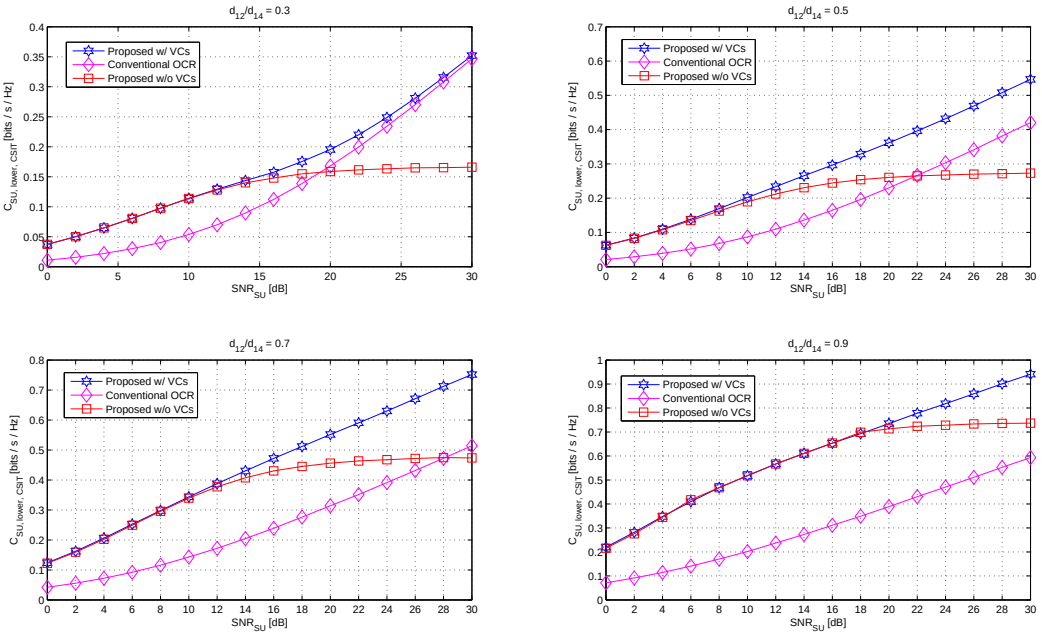

Figure 5. $\mathsf{C}_{\mathrm{SU,lower,CSIT}}$ versus $\mathsf{SNR}_{\mathrm{SU}}$ for different values of d_{12}/d_{14} ($\mathsf{P}_{\mathrm{SU}}/\mathsf{P}_{\mathrm{PU}} = 1$ and CSI at the STx).

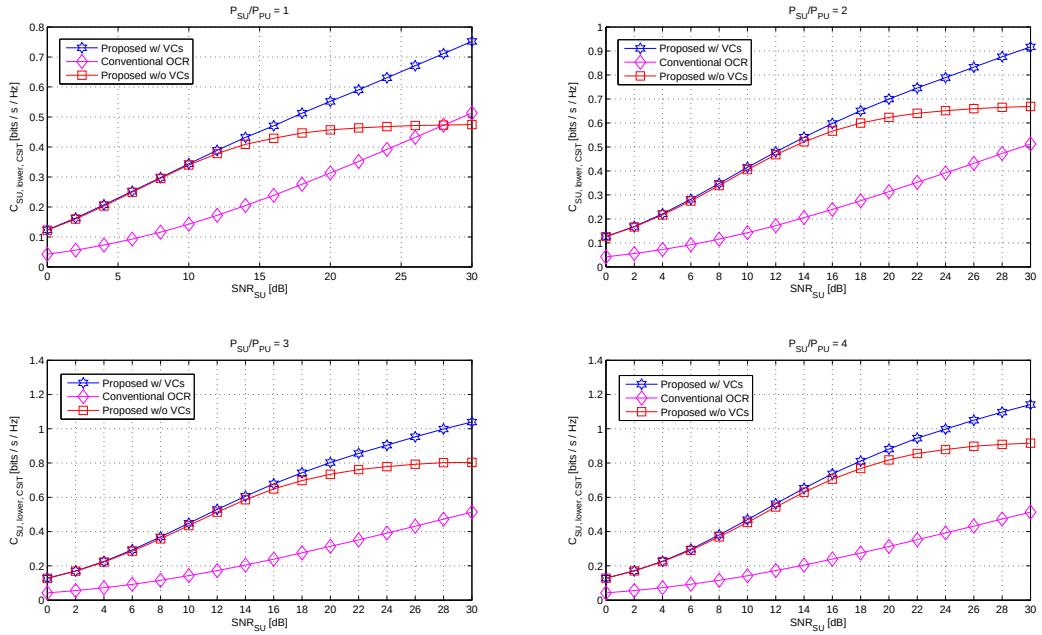

Figure 6. $\mathsf{C}_{\mathrm{SU,lower,CSIT}}$ versus $\mathsf{SNR}_{\mathrm{SU}}$ for different values of $\mathsf{P}_{\mathrm{SU}}/\mathsf{P}_{\mathrm{PU}}$ ($d_{12}/d_{14} = 0.7$ and CSI at the STx).

Figs. 5 and 6, as well as the case in which the STx has no CSI by reporting $\mathsf{C}_{\mathrm{SU,lower,NOCSIT}}$ in Figs. 7 and 8. In both cases, we compare two different implementations of the proposed method: in the former one, referred to as "Proposed w/ VCs", according to (9), the SU transmits on both

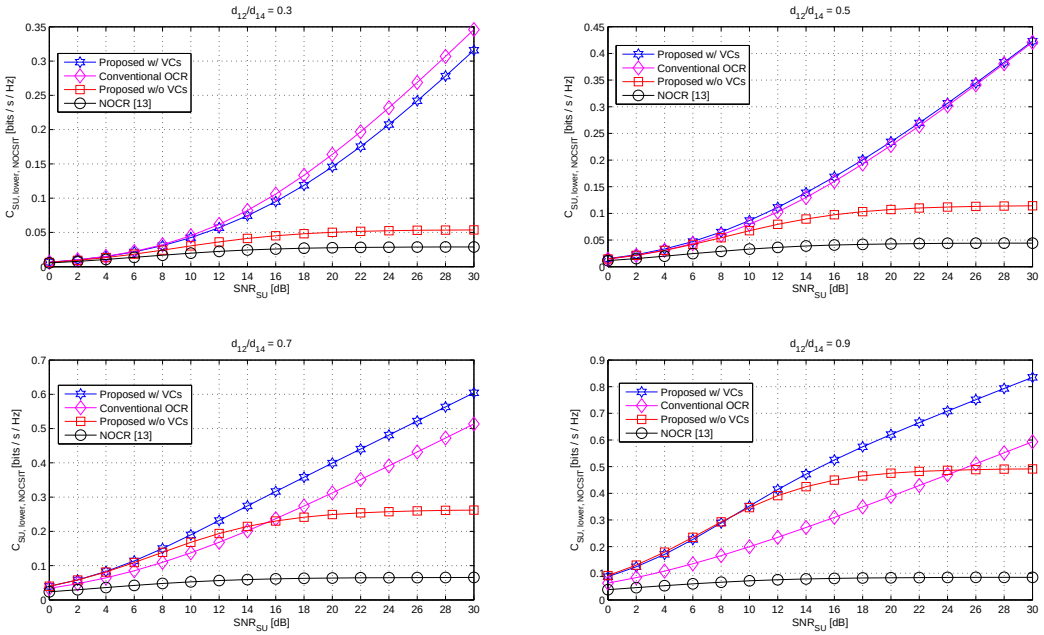

Figure 7. $\mathsf{C}_{\mathrm{SU,lower,NOCSIT}}$ versus $\mathsf{SNR}_{\mathrm{SU}}$ for different values of d_{12}/d_{14} ($\mathsf{P}_{\mathrm{SU}}/\mathsf{P}_{\mathrm{PU}} = 1$ and no CSI at the STx).

the used and virtual subcarriers of the PU; in the latter one, referred to as "Proposed w/o VCs", the SU sends its symbols only over the used subcarriers of the PU, i.e., $\boldsymbol{\mathcal{G}} = \mathbf{O}_{M \times M_{\mathrm{vc}}}$ in (9). Additionally, as a performance comparison, we report the exact ergodic capacity $\mathsf{C}_{\mathrm{PU,direct}}$ of the OCR scheme, referred to as "Conventional OCR", when the SU transmits only on the VCs of the PU, i.e., $\widetilde{\mathbf{F}}(n) = \mathbf{O}_{P \times P}$ in (9); we also plot the worst-case capacity of the NORC scheme [13] when no CSI is available, referred to as "NOCR [13]", which is obtained from (9) by setting $L_{\mathrm{SU}} = 0 \Rightarrow N = 1$, $\boldsymbol{\mathcal{G}} = \mathbf{O}_{M \times M_{\mathrm{vc}}}$, and $\boldsymbol{\mathcal{A}} = \sqrt{a}\,[1, \ldots, 1]^{\mathrm{T}} \in \mathbb{R}^{M}$, where a is given by (50) with $g = 0$.

Figs. 5 and 7 depict the capacity performance as a function of $\mathsf{SNR}_{\mathrm{SU}} \triangleq \mathsf{P}_{\mathrm{SU}}/\sigma^2$ for different values of the ratio d_{12}/d_{13}, with $\mathsf{P}_{\mathrm{SU}}/\mathsf{P}_{\mathrm{PU}} = 1$. Results show that, regardless of the availability of CSI at the STx, the performance of the proposed schemes (with and without VCs) rapidly improves when the STx is moving away from the PTx and, at the same time, it is approaching the SRx. This is a consequence of the fact that, when the distance d_{12} between the PTx and the STx tends to be smaller than the distance d_{24} between the STx and the SRx, the signal-to-interference ratio at the SRx increases. The conventional OCR scheme is able to compete with the proposed scheme with VCs only when the interference generated by the PU transmission over the $1 \rightarrow 4$ link dominates the SU signal, i.e., the STx is too close to the PTx and, at the same time, too far from

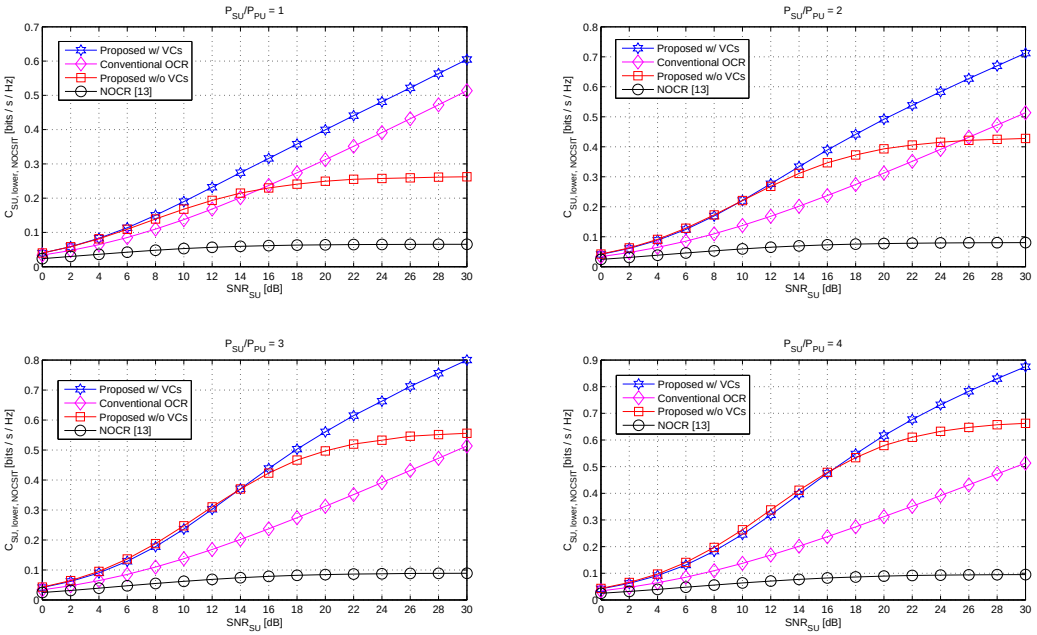

Figure 8. $\mathsf{C}_{\mathrm{SU,lower,NOCSIT}}$ versus $\mathsf{SNR}_{\mathrm{SU}}$ for different values of $\mathsf{P}_{\mathrm{SU}}/\mathsf{P}_{\mathrm{PU}}$ ($d_{12}/d_{14} = 0.7$ and no CSI at the STx).

the SRx. In particular, when $d_{12}/d_{13} = 0.3$, the conventional OCR scheme slightly outperforms the proposed scheme with VCs if there is no CSI at the STx (see Fig. 7). The motivation is that the uniform power allocation is suboptimal (in the information-theoretic sense) for the SU when many subchannels are heavily contaminated by the PU interference. This problem is circumvented if CSI is available at the STx and, hence, power can be optimally allocated on the subcarriers (see Fig. 5). Underneath all of this, it is noteworthy that the OCR scheme necessarily requires the presence of VCs (i.e., spectrum holes) in the PU signal, whose presence might be difficult to reliably detect in practice. In contrast, our scheme can achieve satisfactory data rates even without exploiting the (possible) presence of VCs, especially when the STx is sufficiently close to the SRx. In particular, when $d_{12}/d_{14} > 0.3$, the proposed scheme without VCs ensure a significant increase in data rate with respect to the NOCR scheme proposed in [12], [13] (see Fig. 7), which not only is unable to exploit the presence of the VCs, but also assumes the transmission of one SU symbol per PU data block, i.e, $N = 1$, and does not carry out the precoding of the SU data.

Figs. 6 and 8 report the capacity performance as a function of $\mathsf{SNR}_{\mathrm{SU}}$ for different values of the power ratio $\mathsf{P}_{\mathrm{SU}}/\mathsf{P}_{\mathrm{PU}}$, with $d_{12}/d_{14} = 0.7$. Overall, it is evident that, compared to the other considered schemes, the performance advantage offered by the proposed scheme (with and without VCs) becomes more and more marked when $\mathsf{P}_{\mathrm{SU}}/\mathsf{P}_{\mathrm{PU}}$ increases. We remember that an increase

in the power ratio $\mathsf{P}_{\text{SU}}/\mathsf{P}_{\text{PU}}$ is also beneficial for the PU system (see Fig. 4).

For example, with reference to a primary Wi-Fi system with $1/T_c = 20$ MHz, when $\mathsf{P}_{\text{PU}} = \mathsf{P}_{\text{SU}}$, $d_{12}/d_{14} = 0.7$, and $\mathsf{SNR}_{\text{SU}} = 20$ dB, it results from Figs. 5 and 7 that the SU capacity of the proposed scheme with VCs is at least equal to 11 Mbps with CSIT and 8 Mbps with no CSIT, whereas, when P_{SU} is twice P_{PU}, these gains go up at least to 14 Mbps and 10 Mbps (see Figs. 6 and 8), respectively.

VI. Conclusions

We proposed a spectrum sharing scheme which allows the SU to concurrently transmit within the overall bandwidth of the PU system, by generalizing and subsuming as a particular case existing OCR and NOCR approaches. Contrary to the classical NOCR paradigm, a key feature of the proposed scheme is that the concurrent SU transmission improves (rather than degrades) the performance of the PU system, under reasonable conditions. Another remarkable result is that, if the SU is willing to spend extra transmit power, it can obtain a multicarrier link with a significant data rate. Such a performance might be further improved by assuming that the STx has perfect knowledge of the relevant channel parameters, which allows one to use the waterfilling solution for precoding its information-bearing data.

Appendix A
Proof of Lemma 2

Since $\|\boldsymbol{\alpha}_m\|^2$ in (36) is a strictly increasing function of P_{SU}, $\forall m \in \mathcal{M}$. it is sufficient to show that the first-order partial derivative of $\mathsf{C}_{\text{PU,lower}}$ with respect to $\|\boldsymbol{\alpha}_m\|^2$ is non-negative, $\forall m \in \mathcal{M}$. Starting from (28), one has

$$\frac{\partial}{\partial \|\boldsymbol{\alpha}_m\|^2} \mathsf{C}_{\text{PU,lower}} = \frac{\log_2(e)}{M} \sum_{m \in \mathcal{I}_{\text{PU,uc}}} \frac{\partial}{\partial \|\boldsymbol{\alpha}_m\|^2} \mathsf{E}[\Psi(\Gamma_{3,m})] \,. \tag{55}$$

At this point, let $X_m \triangleq (\boldsymbol{\alpha}_m^{\text{H}} \mathbf{x}_{\text{SU,I}})/\|\boldsymbol{\alpha}_m\|$, we can equivalently rewrite (29) as follows $\Gamma_{3,m} = \mathsf{ASNR}_{13,\text{direct}} \left(1 + Z_m \|\boldsymbol{\alpha}_m\|^2 \frac{\sigma_{12}^2}{\sigma_{13}^2}\right) / \left(1 + \|\boldsymbol{\alpha}_m\|^2 \sigma_{23}^2 \frac{\sigma_{v_2}^2}{\sigma_{v_3}^2}\right)$, where the random variable $Z_m \triangleq |H_{23}(m)|^2 \cdot |X_m|^2$ is the product of two independent exponential random variables with mean σ_{23}^2 and 1, respectively, whose probability density function is denoted by $f(z)$. It can be seen [28] that $f(z) \equiv 0$ for $z < 0$, whereas

$$f(z) = \frac{1}{\sigma_{23}^2} \int_0^{+\infty} \frac{1}{x} e^{-\left(\frac{x}{\sigma_{23}^2} + \frac{z}{x}\right)} \mathrm{d}x = \frac{2}{\sigma_{23}^2} K_0\left(\frac{\sqrt{z}}{\sigma_{23}}\right) , \quad \text{for } z \geq 0 \tag{56}$$

where we have also used the result reported in footnote 21. It results that

$$\frac{\partial}{\partial\|\boldsymbol{\alpha}_m\|^2}\,\mathsf{E}[\Psi(\Gamma_{3,m})] = \frac{\partial}{\partial\|\boldsymbol{\alpha}_m\|^2}\int_0^{+\infty}\left[\int_0^{+\infty} e^{-u}\,\psi(\|\boldsymbol{\alpha}_m\|^2,z,u)\,\mathrm{d}u\right] f(z)\,\mathrm{d}z \tag{57}$$

where $\psi(\|\boldsymbol{\alpha}_m\|^2,z,u) \triangleq \ln\left[1+\mathsf{ASNR}_{13,\text{direct}}\left(1+z\,\|\boldsymbol{\alpha}_m\|^2\,\frac{\sigma_{12}^2}{\sigma_{13}^2}\,u\right)/\left(1+\|\boldsymbol{\alpha}_m\|^2\,\sigma_{23}^2\,\frac{\sigma_{v_2}^2}{\sigma_{v_3}^2}\right)\right]$. As a consequence of the Lebesgue's dominated convergence (see, e.g., [33]), we can interchange the order of differentiation and double integration in (57) because it holds that

(i) $\psi(a,z,u)$ is differentiable for any $a>0$, $z\geq 0$, and $u\geq 0$, and it results that

$$\frac{\partial}{\partial a}\psi(a,z,u) = \left(1+\mathsf{ASNR}_{13,\text{direct}}\,\frac{1+z\,a\,\frac{\sigma_{12}^2}{\sigma_{13}^2}}{1+a\,\sigma_{23}^2\,\frac{\sigma_{v_2}^2}{\sigma_{v_3}^2}}\,u\right)^{-1}\mathsf{ASNR}_{13,\text{direct}}\,\frac{z\,\frac{\sigma_{12}^2}{\sigma_{13}^2}-\sigma_{23}^2\,\frac{\sigma_{v_2}^2}{\sigma_{v_3}^2}}{\left(1+a\,\sigma_{23}^2\,\frac{\sigma_{v_2}^2}{\sigma_{v_3}^2}\right)^2}\,u\,; \tag{58}$$

(ii) $e^{-u}\,\frac{\partial}{\partial a}\psi(a,z,u)$ is summable with respect to u in $(0,+\infty)$ $\forall a>0$ e $z\geq 0$;

(iii) the function $f(z)\int_0^{+\infty} e^{-u}\,\frac{\partial}{\partial a}\psi(a,z,u)\,\mathrm{d}u$ is summable with respect to z in $[0,\infty)$ $\forall a>0$.

Since $z\geq 0$, $u\geq 0$, $f(z)\geq 0$, and $e^{-u}>0$, it is readily proven that $\partial/\partial\|\boldsymbol{\alpha}_m\|^2\,\mathsf{C}_{\text{PU,lower}}\geq 0$ and, hence, $\mathsf{C}_{\text{PU,lower}}$ is a monotonically increasing function of P_{SU}, if

$$z\,\frac{\sigma_{12}^2}{\sigma_{13}^2}-\sigma_{23}^2\,\frac{\sigma_{v_2}^2}{\sigma_{v_3}^2}\geq 0 \iff z\geq \sigma_{23}^2\,\frac{\sigma_{13}^2}{\sigma_{12}^2}\,\frac{\sigma_{v_2}^2}{\sigma_{v_3}^2}\,. \tag{59}$$

Since σ_{23}^2 is bounded when $(\sigma_{13}/\sigma_{12})\,(\sigma_{v_2}\sigma_{v_3})\to 0$,[25] when condition (35) holds, inequality (59) is trivially satisfied because it ends up to $z\geq 0$.

ACKNOWLEDGEMENT

The authors would like to thank Prof. Anna Scaglione for the discussion regarding the latency issues of the proposed scheme, which helped us improve an earlier version of the manuscript.

REFERENCES

[1] J.G. Andrews *et al.*, "What will 5G be?," *IEEE J. Select. Areas Commun.*, vol. 32, no. 6, pp. 1065–1082, June 2014.

[2] F. Boccardi, R.W. Heath, A. Lozano, T.L. Marzetta, P. Popovski, "Five disruptive technology directions for 5G," *IEEE Communications Magazine*, vol. 52, no. 2, pp. 74–80, Feb. 2014

[3] S. Haykin, "Cognitive radio: brain-empowered wireless communications," *IEEE J. Select. Areas Commun.*, vol. 23, pp. 201-220, Feb. 2005.

[4] E. Biglieri et al., *Principles of Cognitive Radio*, New York: Cambridge University Press, 2013.

[5] C.-X. Wang *et al.*, "Cellular architecture and key technologies for 5G wireless communication networks," *IEEE Communications Magazine*, vol. 52, no. 2, pp. 122–130, Feb. 2014.

[25] For instance, if $\sigma_{v_2}^2\approx\sigma_{v_3}^2$ and assuming the path-loss model $\sigma_{i\ell}^2=d_{i\ell}^{-\eta}$, it comes from Carnot's cosine law that $\sigma_{23}^2\to\sigma_{13}^2$.

[6] Y.-C. Liang, Y. Zeng, E.C.Y. Peh, and A.T. Hoang, "Sensing-throughput tradeoff for cognitive radio networks," *IEEE Trans. Wireless Commun.*, vol. 7, pp. 1326–1337, Apr. 2008.
[7] W. Yu, A. Sutivong, D. Julian, T.M. Cover, and M. Chiang, "Writing on colored paper", *Proc. of IEEE Int. Symp. Inf. Theory (ISIT)*, Washington, DC, USA, June 2001.
[8] A. Khisti, U. Erez, and G. Wornell, "Writing on many pieces of dirty paper at once: The binary case", *Proc. of IEEE Int. Symp. Inf. Theory (ISIT)*, Chicago, USA, June 2004.
[9] N. Devroye, P. Mitran, and V. Tarokh, "Achievable rates in cognitive radio channels," *IEEE Trans. Inf. Theory*, vol. 52, pp. 1813–1827, May 2006.
[10] A. Jovicic and P. Viswanath, "Cognitive radio: An information-theoretic perspective," *IEEE Trans. Inf. Theory*, vol. 55, pp. 3945–3958, Sep. 2009.
[11] M. Costa, "Writing on dirty paper," *IEEE Trans. Inf. Theory*, vol. 29, pp. 439–441, May 1983.
[12] F. Verde, A. Scaglione, D. Darsena, G. Gelli, "An amplify and forward scheme for cognitive radios", *Proc. of IEEE International Conference on Acoustic, Speech and Signal Processing (ICASSP)*, Florence, Italy, May 2014, pp. 2743-2747.
[13] F. Verde, A. Scaglione, D. Darsena, G. Gelli, "An amplify-and-forward scheme for spectrum sharing in cognitive radio channels", *IEEE Trans. Wireless Commun.*, vol. 14, pp. 5629–5642, Oct. 2015.
[14] C.R. Stevenson *et al.*, "IEEE 802.22: The first cognitive radio wireless regional area network standard," *IEEE Communications Magazine*, pp. 130–138, Jan. 2009
[15] D. Darsena, G. Gelli, F. Verde, "Amplify-and-forward secondary spectrum access in multicarrier cognitive radio systems", *Proc. of the IEEE International Workshop on Measurements and Networking (M&N)*, Coimbra, Portugal, Oct. 2015, pp. 161-166.
[16] E. Biglieri, J.G. Proakis, and S. Shamai, "Fading Channels: Information-Theoretic and Communications Aspects," *IEEE Trans. Inf. Theory*, vol. 44, pp. 2916–2692, Oct. 1998.
[17] R.G. Gallager, *Information Theory and Reliable Communication*, New York: Wiley, 1968.
[18] T.M. Cover and J.A. Thomas, *Elements of Information Theory*, New York: Wiley, 1991.
[19] A. Ben-Israel and T. N. E. Greville, *Generalized Inverses*, New York: Springer-Verlag, 2002.
[20] R. A. Horn and C. R. Johnson. *Matrix Analysis*. Cambridge University Press, 1990.
[21] A. Sabharwal *et al.*, "In-band full-duplex wireless: Challenges and opportunities", *IEEE J. Select. Areas Commun.*, vol. 32, pp. 1637–1652, Sep. 2014.
[22] Z. Wang and G.B. Giannakis, "Wireless multicarrier communications – where Fourier meets Shannon," *IEEE Signal Processing Magazine*, pp. 29–48, May 2000.
[23] M. Morelli and U. Mengali, "A comparison of pilot-aided channel estimation methods for OFDM systems," *IEEE Trans. Signal Process.*, pp. 3065–3073, Dec. 2001.
[24] D. Darsena, G. Gelli, L. Paura, F. Verde, "A constrained maximum-SINR NBI-resistant receiver for OFDM systems," *IEEE Trans. Signal Process.*, vol. 55, pp. 3032-3047, June 2007.
[25] D. Darsena, G. Gelli, F. Melito, F. Verde, "ICI-free equalization in OFDM systems with blanking preprocessing at the receiver for impulsive noise mitigation", *IEEE Signal Process. Lett.*, vol. 22, pp. 1321-1325, Sep. 2015.
[26] R.M. Gray, "Toeplitz and circulant matrices: A review," *Foundations and Trends in Communications and Information Theory*, vol. 2, issue 3.
[27] L. Ozarow, S. Shamai, and A. Wyner, "Information theoretic considerations for cellular mobile radio," *IEEE Trans. Veh. Technol.*, vol. 43, pp. 359 – 378, May 1994.
[28] A. Papoulis. *Probability, Random variables, and Stochastics Processes (3rd ed.)*. McGraw-Hill, Singapore, 1991.
[29] *Handbook of Mathematical Functions with Formulas, Graphs, and Mathematical Tables*, Edited by M. Abramowitz and I.A. Stegun, National Bureau of Standards, 1972.
[30] A.P. Prudnikov, Y.A. Brychkov, and O.I. Marichev, *Integrals and Series*, Vol. 1, Gordon and Breach Science Publishers, Amsterdam, 1986.
[31] T.M. Cover and J.A. Thomas, "Determinant inequalities via information theory," *SIAM J. Matrix Anal. Appl.*, vol. 9, pp. 384–392, July 1988.
[32] D. Tse and P. Viswanath, *Fundamentals of Wireless Communication*, Cambridge University Press, 2005.
[33] W. Rudin, *Principles of Real Analysis*, McGraw-Hill, New York, 1976.